AWPHM
T564
1987

INCLUSION COMPLEX FORMATION BETWEEN α–CYCLODEXTRIN AND SYMMETRICAL 4,4'–DISUBSTITUTED BIPHENYL COMPOUNDS

BY

DAVID TOLEDO–VELASQUEZ

A thesis submitted in partial fulfillment of the
requirements for the degree of

MASTER OF SCIENCE
(PHARMACY)
at the
UNIVERSITY OF WISCONSIN–MADISON
1987

APPROVED:

K. A. Connors — June 19, 1987 (date)

J. Wright — June 19 1987 (date)

G. Zografi — June 19, 1987 (date)

Pharmacy
AWM
T564

To my mother Aurora, my father Fernando, and to my brothers Antonio and Fernando; their love, support, and encouragement gave me the confidence and the will to pursue graduate education.

ACKNOWLEDGEMENTS

I wish to thank Dr. Kenneth A. Connors for his patient guidance and suggestions throughout the course of this investigation. The breadth and clarity of his thinking have been the greatest influence on my graduate education.

I also thank Andrea Paulson for her contributions of data, programming and discussion.

My appreciation is extended to the Mexican Government for the financial support provided through the National University of Mexico, FES-Cuautitlan, and the National Council of Science and Technology, CONACYT.

TABLE OF CONTENTS

INCLUSION COMPLEX FORMATION BETWEEN α–CYCLODEXTRIN AND SYMMETRICAL 4,4'–DISUBSTITUTED BIPHENYL COMPOUNDS

David Toledo–Velasquez

(Under the supervision of Professor Kenneth A. Connors)

Complex formation of α–cyclodextrin and sym-1,4–disubstituted benzenes was previously studied in this laboratory. The calculation of the stability constants was made by assuming that two complexes were formed, namely SL and SL_2, characterized by different microscopic binding constants. The experimental measured stability constants K_{11} and K_{12}, based on the context of symmetrical disubstituted substrates, are related to the microscopic binding constants by $K_{11} = 2\,K_{X'X}$ and $K_{12} = a_{XX}\,K_{11} / 4$, where $a_{XX} = K_{X'X'} / K_{X'X}$ by definition. Thus, a_{XX} represents the extent of interaction between binding sites.

The benzene series gave information about the interaction between the two substrate binding sites in the 1:2 complex. In particular, the a_{XX} values clearly were strongly influenced by the proximity of the two binding sites. A logical step is therefore to increase the distance between the sites. The benzene series also showed an inverse relationship between the binding constant K_{11}

and the intrinsic solubility S_o. This relationship was described by the equation

$$\log K_{11} = -0.59 \log S_o + 0.40$$

In this work, sym-4,4'–disubstituted biphenyls were studied in aqueous solution at 25 °C. These substrates were chosen because they provide an increased distance between binding sites while keeping the sites electronically linked as in the benzene series. The binding constants K_{11}, K_{12}, and a_{XX} were determined under the same experimental conditions. The data were interpreted using the binding site model previously described. The following results were obtained:

1. All the substrates except the 4,4'-dicarboxybiphenyl followed the binding model assumed. The latter substrate was found to follow a model where $K_{12}>>>K_{11}$ so no SL is detectable and the detectable complex is present as SL_2, with $\beta_{12} = K_{11}K_{12} = 2.9 \times 10^7\ M^{-2}$.

2. It was found that a plot of $\sqrt{S_t}$ against L_t provides a useful extrapolation estimate of the intrinsic solubility S_o.

3. A good correlation was observed between substrate dissolution process and the binding process when the model (solubility) process and the binding process involve only K_{11} binding. The relationship between K_{11} and S_o for the biphenyl series is given by the following equation

$$\log K_{11} = -0.578 \log S_o - 0.66$$

4. The slopes of the equations that relate K_{11} and S_o in the benzene and biphenyl series were not significantly different at the 95 % confidence level. This correlation is an indication of a similarity between solubility model and the binding process for the biphenyl and the benzene series.

Approved: Kenneth A. Connors

Kenneth A. Connors

June 19, 1987

date

I. INTRODUCTION

In 1891 Villiers isolated a family of non-reducing oligomers produced by the enzymatic action of amylases of Bacillus macerans on starch (1). However, it was not until the early 1900's that Schardinger (2) elucidated the general structure of these compounds, showing them to be cyclic oligosaccharides. Cyclodextrins are well known to form inclusion complex with a variety of organic molecules and this characteristic has attracted interest in many fields, specially as a model for studies of enzyme -substrate interaction (3). Also, cyclodextrins have potential widespread utilization in the pharmaceutical, food, chemical, and other industries (4). The literature contains references to the chemistry, production, and purification of cyclodextrins (5-8) as well as recent reviews (9-10).

A. Structure and Properties of the Cyclodextrins

Cyclodextrins or cycloamyloses are composed of D(+) - glucopyranose units connected by $\alpha(1,4)$ linkages, leading to the overall shape of a toroidal truncated cone with a central void. Since the enzymatic action of the amylases is not very specific, it is possible to find cyclic oligosaccharides

containing different numbers of D(+) - glucopyranose units. However, cycles composed of less than six members are not possible because of the excessive steric strain (11) and also because of the sixfold character of the starch helix (12). On the other hand, higher cycles composed of up to twelve glucose units are difficult to obtain in suitable quantities. Those consisting of six, seven, and eight D(+) - glucopyranose units are called α–, β–, γ–cyclodextrin, respectively. Alternatively they are name cyclohexaamylose, cycloheptaamylose, and cyclooctaamylose. The molecular structure of α-cyclodextrin is given in scheme I and the cyclodextrins' most important physical characteristics are given in Table I. With respect to the stereochemistry of the cyclodextrins, proton magnetic resonance spectra of α-cyclodextrin in deuterium oxide solution (13,14,15) as well as X-ray crystallography studies (16) have established the C-1 chair conformation for the D(+) -glucopyranose units. This uniform stereochemistry provides to the cyclodextrin a wider side formed by twelve secondary hydroxyl groups from positions 2 and 3 of the glucose unit and a narrow side formed by six primary hydroxyl groups from position 6 of the glucose unit. The primary hydroxyl groups can rotate and partially block the narrow end of the cavity, unlike the secondary hydroxyl groups, which are rigidly held by the existence of hydrogen bonding on C-2 and C-3 atoms of adjacent D(+) - glucopyranose units (17,18). This rigidity of the secondary hydroxyl groups stabilizes the ring and keeps the diameter of the wider end of

Scheme I. Structure of α–Cyclodextrin

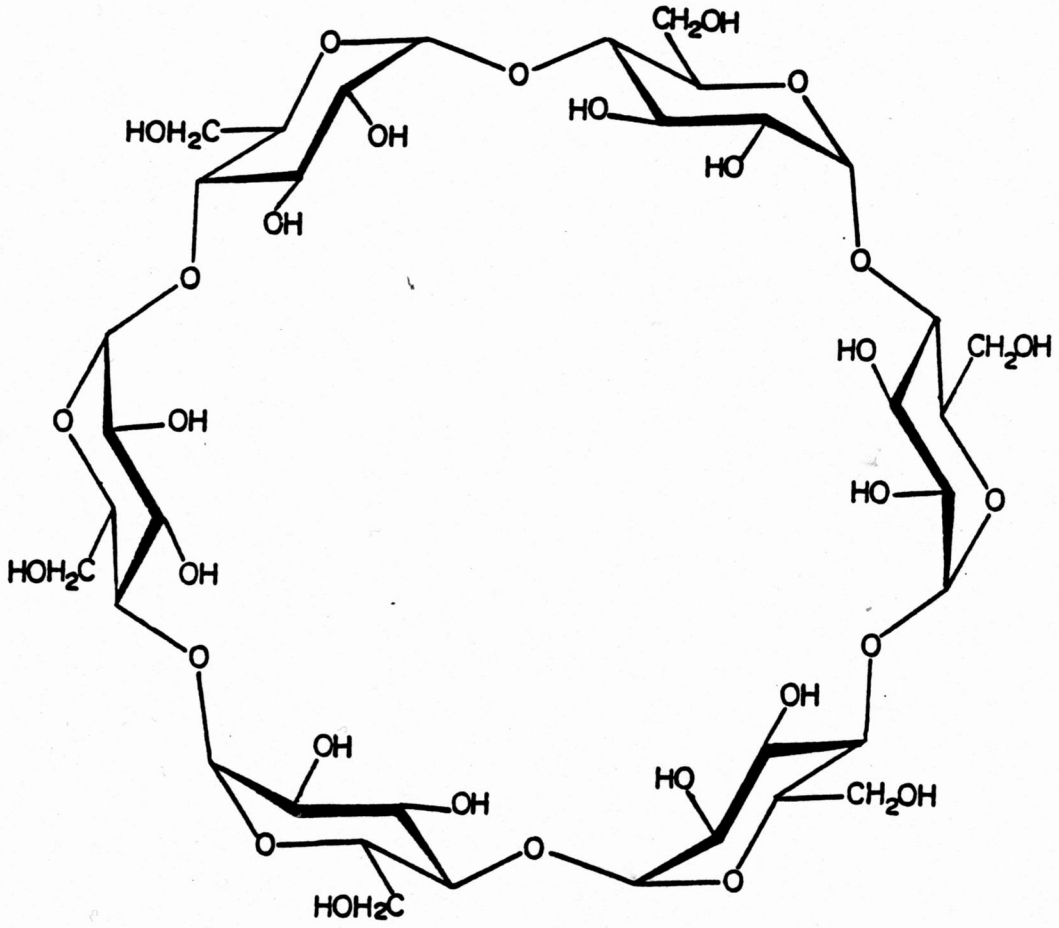

Table I. Some Physical Properties of Cyclodextrins

Cyclodextrin	Number of Glucose units	Molecular weight	Specific [a] rotation $[\alpha]_D$ / Deg.	Solubility [b] in water (25 °C) (g/100ml)	Cavity size (Å) Internal Diameter	Cavity size (Å) Depth
α	6	972	150.5 ± 0.5	11.78	4.7 [c] 6.0 [d] 4.7 [e]	6.7 [c]
β	7	1135	162.5 ± 0.5	1.85	6.0–6.4 [e] 8.0 [d]	7.0 [f]
γ	8	1297	177.4 ±0.5	21.76	7.5–8.3 [e] 10.0 [d]	7.0 [f]

a. ref. 19
b. ref. 20
c. ref. 21
d. ref. 22
e. ref. 23
f. ref. 7

the cavity relatively constant. The existence of these hydroxyl groups occupying both rims gives to the exterior of the cyclodextrin a hydrophilic character. Conversely, the central void part of the cyclodextrin is relatively hydrophobic in character due to the projection of hydrogens from positions 3 and 5 and also the existence of the ether-like oxygens from position 4. One of the most important characteristics of the cyclodextrin is associated with its relative hydrophilic and hydrophobic character. Thus, in solution, the cyclodextrin cavity provides a hydrophobic matrix in a hydrophilic surroundings. The cavity of cyclodextrins is not empty in aqueous solution. Thermodynamic studies (24) have indicated that α-cyclodextrin is able to form different hydrates. Some of these hydrates have been studied crystallographically (25,26). In α-cyclodextrin hexahydrate four of the six water molecules of hydration are located outside the α-cyclodextrin. The other two water molecules are hydrogen bonded to one another and are enclosed in the cyclodextrin cavity. Also, one of the enclosed water molecules is hydrogen bonded to two hydroxyl groups from position 6 of the D(+) - glucopyranose units (25). These structural characteristics have formed the basis for a postulated mechanism of inclusion compound formation (27).

B. Inclusion Complex Formation

1. Structure and Binding in Cyclodextrin Complexes.

One of the interesting characteristics of the cyclodextrins is their ability to form inclusion complexes, with a variety of compounds, in their cavities. The most important parameters that determine the stability of the complex of a given molecule are its hydrophobicity, relative size, geometry, and deepness of penetration in relation to the cyclodextrin cavity (28,29).

Direct evidence verifying inclusion of a molecule within the cavity of cyclodextrin was first obtained from the three-dimensional x-ray diffraction data of the potassium acetate complex of cyclohexaamylose (16), and later from crystallographic characteristics of a variety of 1:1 complexes (30). Demarco and Thakkar (31) investigated the proton magnetic resonance of the complex formation of cycloheptaamylose and p-hydroxybenzoic acid and other guest molecules and established that the formation of inclusion complexes appears to occur also in solution. Many other studies have confirmed these findings (32-35). As a result, investigators have searched for factors controlling the complex formation. The literature frequently refers to noncovalent attractive forces and driving forces. It is important to notice that driving forces are a consequence of the attractive forces and the interaction among the substrate, ligand, and medium (solvent). Noncovalent attractive forces are of three types:

electrostatic, induction, and dispersion . The specific driving forces that have been invoked involve release of enthalpy-rich water from the cyclodextrin cavity (32,36a), relief of cyclodextrin strain energy (25),and hydration of the complex (36b). The driving forces have been described (37a) conveniently as the overall free energy change for the complexation process in which medium-medium interactions, medium-solute interactions, and solute-solute interactions are taken into account.

2. Stoichiometric relationships in complexation

One of the primary pieces of information, prior to designing a model and evaluating binding constants, is the stoichiometric relationship of the system. The literature describes different techniques for the evaluation of stoichiometry (37b,38).

The complex formation of substrate (S) and ligand (L) can be represented by the following expression

$$mS + nL \rightleftharpoons S_m L_n$$

where m and n are the stoichiometric coefficients, S represents substrate (ex. disubstituted biphenyl), and L represents the ligand (ex. α-cyclodextrin). Thus, the overall binding constant can be defined as:

$$\beta_{mn} = \frac{[S_m L_n]}{[S]^m [L]^n}$$

where brackets signify molar concentrations.

Values of integers greater than one for m or n imply the existence, for the substrate or the ligand, of more than one binding site (37c). If for the complex formation the existence of stepwise reactions is assumed, then there is a K_{hi} stepwise constant for each complexation step. This is the case in the present work, in which the system contains two stoichiometric binding constants, K_{11} and K_{12}, because of the existence of 1:1 and 1:2 substrate-cyclodextrin complexes. The stepwise binding constants can be defined from the stepwise equilibria:

$$L + S \rightleftharpoons SL$$

$$K_{11} = \frac{[SL]}{[L][S]}$$

$$SL + L \rightleftharpoons SL_2$$

$$K_{12} = \frac{[SL_2]}{[SL][L]}$$

where brackets indicate molar concentration of the complexes (SL_2, SL), free substrate (S), and free ligand (L). The stoichiometric binding constants K_{11} and K_{12} are described in this work as binding or stability constants.

II. RESEARCH PLAN

A. Binding Model

Previous studies (39,40,41) have described the stoichiometry as well as a binding model for the interpretation of binding constants. This model can be represented by scheme II as described by Rosanske and Connors (39).

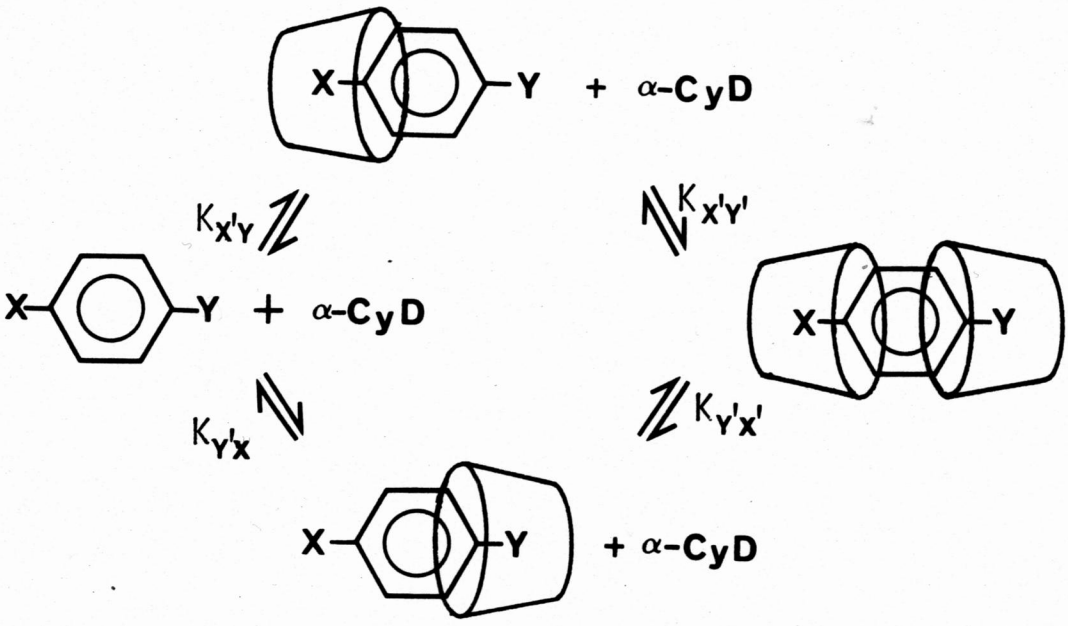

Scheme II

It has been assumed that the disubstituted compound is a two-site substrate (sites X and Y) and α-cyclodextrin is a one-site ligand, only one end of the cavity being entered by the substrate. For the scheme being considered the leading substituent, X or Y, represents the site that was first bound and the superscript prime indicates a site bound by ligand. Thus, there exist two isomeric 1:1 complexes and one 1:2 complex. The formation of these complexes is characterized by different microscopic binding constants.

The experimentally measured stability constants K_{11} and K_{12} are related (39) to the microscopic binding constants by equations 1 and 2,

$$K_{11} = K_{X'Y} + K_{Y'X} \qquad \text{eq. 1}$$

$$K_{12} = \frac{K_{X'Y'}\, K_{Y'X'}}{K_{X'Y'} + K_{Y'X'}} \qquad \text{eq. 2}$$

The extent of interaction between the two sites in 1:2 complex formation has been defined (40) by the interaction parameter a_{XY}, which expresses a ratio of microscopic binding constants for the following reaction:

$$X'Y + Y'X \rightleftharpoons X'Y' + XY$$

$$a_{XY} = \frac{K_{X'Y'}}{K_{Y'X}} = \frac{K_{X'Y'}}{K_{X'Y}} \qquad \text{eq. 3}$$

Combination of the previous equations gives equation 4.

$$K_{12} = \frac{a_{XY} K_{X'Y} K_{Y'X}}{K_{X'Y} + K_{Y'X}} = \frac{a_{XY} K_{X'Y} K_{Y'X}}{K_{11}} \qquad \text{eq. 4}$$

Note that eqs. 1 and 4 constitute two independent equations with three unknown quantities, namely $K_{X'Y}$, $K_{Y'X}$, and a_{XY}.

In order to evaluate the microscopic binding constants and the interaction parameter, we will make use of the special case in which the two substrate binding sites are identical, then X = Y, $K_{X'Y} = K_{Y'X}$, and equations 1 and 4 become:

$$K_{11} = 2 K_{XX} \qquad \text{eq.5}$$

$$K_{12} = \frac{a_{XX} K_{11}}{4} \qquad \text{eq. 6}$$

Thus the parameters K_{XX} and a_{XX} can be evaluated using eq. 5 and 6. This special case was used in previous work done by Pendergast and Connors (41) and will be used in the present study.

B. Complexation Results of α -Cyclodextrin with Sym- 1,4- Disubstituted Benzenes

Pendergast in previous studies (42) determined the stability constants for α-cyclodextrin complexes with sym - 1,4 - disubstituted benzenes. The results are listed in Table II, which includes K_{11}, K_{12}, the interaction parameter a_{XX}, and the intrinsic solubility values S_o for the substrates. The understanding of the complexing behavior and the interpretation of the stability constants were done with the aid of postulates based on previous systematic studies of substrate structure - complex stability relationships (40,43,44). It has been postulated that cyclodextrin complex stability in aqueous solutions

1. Decreases with increase in substrate site polarity;
2. Increases with increase in substrate site electron density;
3. Increases with increase in substrate site polarizability.

Several empirical correlations were obtained in Pendergast's work. First, according to the electronic distribution of the symmetrical substrates in their resonance forms (scheme III), there exist two extremes because of the presence of either electron-donating substituent, form 1, or electron-withdrawing substituent, form 3. These extremes have significant charge

Table II

Stability Constants for α - Cyclodextrin Complexes with Sym- 1,4-Disubstituted Benzenes, X–C_6H_4–X, at 25 °C in 0.1 M NaCl[a]

X	$10^4 S_o$ / M	K_{11} / M^{-1}	K_{12} / M^{-1}	a_{XX}
OCH_3	55.3	75.4	221	11.7
OC_2H_5	4.56	128	326	10.2
I	0.031	5060	6250	4.94
Br	0.59	913	397	1.74
Cl	3.99	232	90	1.55
COOH	0.192[b]	1344	23.8	0.071
$COOCH_3$	1.69	464	109	0.93
$COCH_3$	38.9	10.2	0	
CN	6.97	33.1	7.2	0.87
NO_2	2.35	35.8	4.6	0.51

a. Ref. 42
b. In 0.10 M HCl

Scheme III

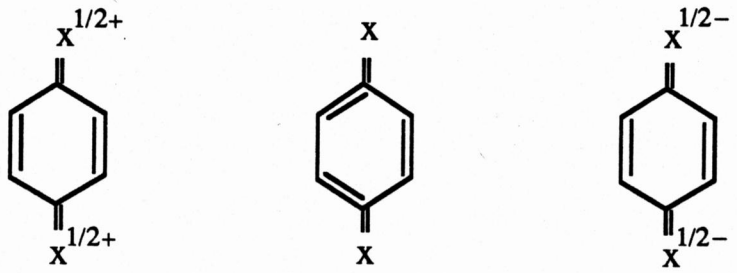

1 2 3

separation producing high binding site polarity, thus from postulate 1 there will be a decrease in complex stability. This pattern was observed with substituents having large absolute values of the Hammett constant σ.

Second, Pendergast found an inverse relationship between K_{11} and S_o. A linear relationship was observed for most of the ten substituents (see figure 1), the equation of the line being

$$\log K_{11} = -0.59 \log So + 0.40$$

The substrates that did not follow the correlation (X = NO_2, CN, $COCH_3$) have high group (site) dipole moments and had log K_{11} values lower than predicted. A good correlation for all the substrates was obtained by performing a multiple linear regression on log S_o and group dipole moment of

the substrate, μ. The correlation equation is :

$$\log K_{11} = - 0.636 \log S_o - 0.231 \mu + 0.524 \qquad (r = 0.94)$$

The correlation between K_{11} and S_o suggests that there is a possibility of a relationship between the inclusion complexation and the solubility process.

Pendergast also found that the interaction parameter a_{XX} is very dependent on the nature of the substituent binding site, being apparently sensitive to the substituent electron-withdrawing or electron-donating ability. The values of a_{XX} for the benzene series range from 0.07 to 11.7 . Thus these systems showed both competitive and cooperative behavior between the binding sites. Note that if the two sites are completely independent a_{XX} should be equal to one. It seems chemically reasonable that a major determinant of a_{XX} should be the distance between the binding sites.

Figure 1

Plot of log K_{11} versus log S_o for ten symmetrical 1,4- Disubstituted Benzenes. The straight line was computed using linear regression for the seven substrates with the highest K_{11} values (Ref. 42).

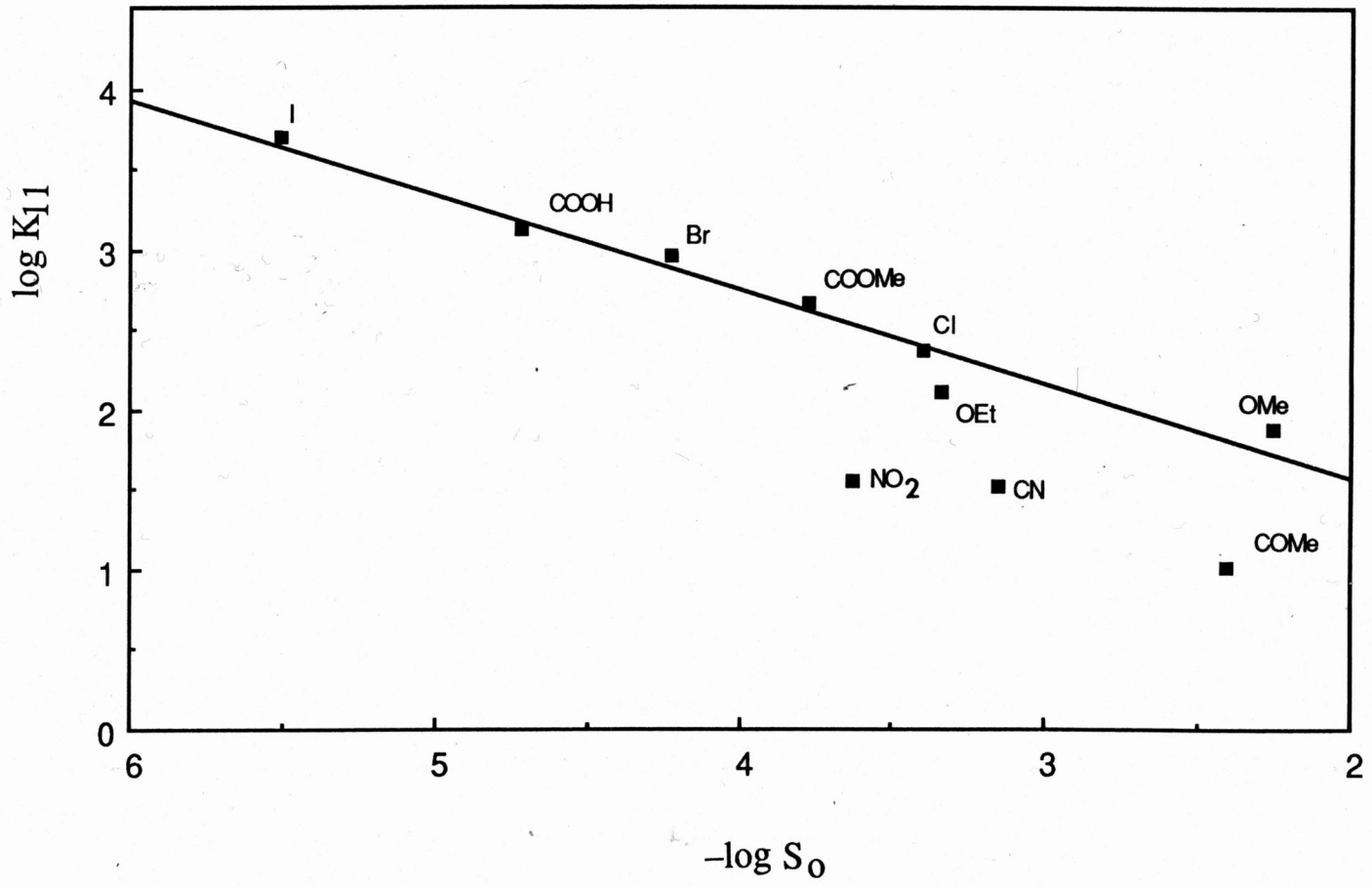
log K_{11}
4
3
2
1
0
6
5
4
3
2
–log S_o
I
COOH
Br
COOMe
Cl
OEt
NO_2
CN
OMe
COMe

C. Objectives

Pendergast's study of sym-1,4–disubstituted benzenes gave information about the dependence of stability constants on structure and about the interaction between the two substrate binding sites in the 1:2 complex. In particular, the a_{XX} values clearly were strongly influenced by the proximity of the two binding sites. A logical step is therefore to increase the distance between the sites while keeping other disubstituted benzene features constant. It was therefore decided to study the complexation process of α–cyclodextrin with sym-4,4'–disubstituted biphenyls. These substrates were chosen because they have two binding sites which are connected by a conjugated portion so the binding sites are electronically linked as in Pendergast's work. The relationship of these two series is shown in these structures:

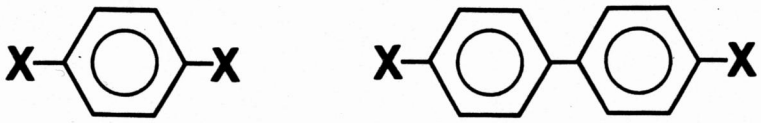

This study was a collaborative effort by the present writer and Ms. A. Paulson of this laboratory. The specific objectives of this thesis were to obtain quantitative information of the binding constants on four of the substartes chosen for the study, to interpret the binding constant data, and to examine the substrate dissolution process as a model for binding processes. The interpretation was done using the entire set of substrates.

III. EXPERIMENTAL METHODS

A. Determination of Binding Constants

Some experimental methods for the study of binding constants are briefly described in Table III (37d).

The properties of the substrates in this study, disubstituted biphenyls, led to the choice of the solubility method for the binding constant determination. Some of the other methods are not applicable because of the low solubility and non-ionizable nature of the biphenyls. The solubility method is appropriate for compounds with low aqueous solubility. Moreover, the constants for both 1:1 and 1:2 binding can be estimated by means of mathematical treatments described in the literature.

B. Theory of the Solubility Method

In this method the free substrate concentration was fixed at S_o, the equilibrium solubility, by having an excess of solid substrate. The apparent total solubility of a substrate, S_t, was measured as a function of the total ligand (cyclodextrin) concentration, L_t. The mathematical treatment that describes the formation of complexes SL and SL_2 has been described by Higuchi and Kristiansen (45), and Kakemi and coworkers (46).

Table III. Experimental methods for the study of binding constants

Method	Bases
Chromatography	Change in observed retention time upon formation of the complex.
Dialysis	Two compartments are separated by a semipermeable membrane. Difference in molecular size of the substrate and ligand provides the basis for the evaluation of the complex.
Liquid-liquid partitioning	From partition isotherm studies and the use of the apparent partition coefficient,it is possible to evaluate the extent of binding.
Magnetic resonance spectroscopy	Change in chemical shift upon complexation as a result of shielding effects of the ligand.
Optical absorption spectroscopy	Measure of the significant spectral changes as a consequence of complex formation.
Potentiometry	Based on the change in concentration of ionic species as a consequence of complexation equilibrium.
Reaction kinetics	The substrate chemical reactivity, as expressed quantitatively in a rate constant, is altered upon complexation.
Solubility	The apparent solubility is altered due to the complex formation. Thus, it is possible to evaluate the equilibrium constant from solubility data.

Thus, there exist two equilibria as follows:

$$S + L \rightleftharpoons SL$$

$$SL + L \rightleftharpoons SL_2$$

And the stability constants are given by:

$$K_{11} = \frac{[SL]}{[L][S]} \qquad \text{eq. 7}$$

$$K_{12} = \frac{[SL_2]}{[SL][L]} \qquad \text{eq. 8}$$

The mass balance equations are:

$$S_t = [S] + [SL] + [SL_2] \qquad \text{eq. 9}$$

$$L_t = [L] + [SL] + 2[SL_2] \qquad \text{eq.10}$$

By combining equations 7 - 10 and since $[S] = S_o$, the mass balance equations become:

$$S_t = S_o + K_{11}S_o[L] + K_{11}K_{12}S_o[L]^2 \qquad \text{eq.11}$$

$$L_t = [L] + K_{11}S_o[L] + 2K_{11}K_{12}S_o[L]^2 \qquad \text{eq.12}$$

Equation 11 can be rearranged to

$$\frac{S_t - S_o}{[L]} = K_{11}S_o + K_{11}K_{12}S_o[L] \qquad \text{eq.13}$$

From equation 13 a plot of $(S_t - S_o) / [L]$ versus $[L]$ gives both K_{11} and K_{12} from the intercept and the slope, respectively. However, free ligand concentration, $[L]$, is not known. Solving for $[L]$ from the quadratic equation 12, we have:

$$[L] = \frac{-(K_{11}S_o + 1) + \{(K_{11}S_o + 1)^2 + 8K_{11}K_{12}S_oL_t\}^{1/2}}{4K_{11}K_{12}S_o}$$

eq. 14

where the positive root has been used. Thus $[L]$ can be calculated from equation 14, then used in equation 13 to obtain K_{11} and K_{12} values. The procedure involves an iterative process until constant values for the stability constants are obtained. It is necessary, however, to have initial estimates of K_{11} and K_{12}. To obtain these, the approximation $[L] = L_t$ was made. Therefore, equation 13 becomes, approximately,

$$\frac{S_t - S_o}{L_t} = K_{11}S_o + K_{11}K_{12}S_oL_t \qquad \text{eq.15}$$

Thus, from a plot of $(S_t - S_o) / L_t$ versus L_t the first estimates for K_{11} and K_{12}, can be calculated.

C. Data Treatment

The K_{11} and K_{12} values are obtained from the slope and the intercept of the linear plot of equation 13. An unweighted least squares analysis was used for the estimation of the slope, the intercept, and their variances. Unweighted analysis can be used (37) when:

a. $\sigma_{xi} <<< \sigma_{yi}$, or

b. σ_{yi} is independent of i

where σ_x is the variance of the independent variable and σ_y is the variance of the dependent variable. Estimates of the independent and dependent variances were obtained from preliminary studies of 1,4-dimethylterephtalate system. Substrate concentrations (1,4-dimethylterephtalate) were determined as a function of nine different α-cyclodextrin (ligand) concentrations. The variance of the ligand concentration was assumed to be negligible compared to the

variance of the substrate concentration . The relative variance of the substrate plotted against the ligand concentration was shown to be independent of the abscissa error. Therefore, unweighted least square analsis can be used. The variances of the constants K_{11}, K_{12}, and a_{xx} were obtained by a propagation of errors treatment according to equation 16

$$\sigma_y^2 = \left(\frac{\partial F}{\partial x_1}\right)^2 \sigma_{x_1}^2 + \left(\frac{\partial F}{\partial x_2}\right)^2 \sigma_{x_2}^2 + \ldots\ldots \qquad \text{eq.16}$$

where $y = f(x_1, x_2, \ldots)$. The specific equations for the variance of K_{11}, K_{12}, and a_{XX} are given by equations 17, 18, and 19, respectively.

$$\sigma_{K_{11}}^2 = \frac{\sigma_{S_o}^2}{S_o^2} K_{11}^2 + \frac{\sigma_b^2}{b^2} K_{11}^2 \qquad \text{eq.17}$$

$$\sigma_{K_{12}}^2 = \frac{\sigma_b^2}{b^2} K_{12}^2 + \frac{\sigma_m^2}{m^2} K_{12}^2 \qquad \text{eq.18}$$

$$\sigma_{a_{xx}}^2 = \frac{\sigma_{K_{11}}^2}{K_{11}^2} a_{xx}^2 + \frac{\sigma_{K_{12}}^2}{K_{12}^2} a_{xx}^2 \qquad \text{eq.19}$$

All the least squares analysis of equation 13 as well as the determination of the first estimates, using equation 15, of the stability constants K_{11} and K_{12}, were performed by computer. The programs (BASIC language) (47) are reproduced in appendix A.

D. Materials

α-Cyclodextrin obtained from Sigma Chemical Co. was used in all the experiments without further purification. Previous experiments (42) have shown equivalent results when using recrystallized and unrecrystallized α-cyclodextrin from Sigma. The substrates used, their sources, purification process, as well as observed and literature melting points are described in Table IV. All solutions were prepared with ion-exchanged water redistilled from alkaline permanganate. Methanol A.C.S. grade from Fisher Scientific or N, N-dimethylformamide (DMF) from Aldrich (double distilled) in appropriate dilution was used for dilutions prior to spectophotometric analysis. All other chemicals used were analytical grade.

TABLE IV. Identification of Substrate Materials
sym - $X-C_6H_4-C_6H_4-X$

X	SOURCE	RECRYS-TALIZATION SOLVENT	MELTING POINT (°C)		Ref.
			OBSERVED	LITERATURE	
Br	Aldrich	CH_3OH	166.5 - 168	163 - 164	48
				166.5 - 167	49
COOH	Pfaltz and Bauer	a	———	b	50
CN	Eastman	CH_3OH	237	237	51
NO_2	Tokyo Kasei Kogyo	CH_3OH	238	239 - 239.5	49

a. Not recrystallized
b. Does not melt or sublime

E. Equipment

Substrates as well as α-cyclodextrin were dried for 3 hours at 105 °C using a Huppert's oven KH1200 (K.H. Huppert Co., Chicago, Il). Melting points were determined with a Thomas capillary melting point apparatus (Arthur H. Thomas Company, Philadelphis, PA). A water bath at 25.0 ± 0.1 °C with a rotating sample holder (32 rpm) was used for the temperature equilibrium process. Filtration of samples was done by using 0.2 micron Teflon® membrane filters TF-200 (Gelman Instrument Co., Ann Arbor, MI) contained in 25mm millipore swag-lok filter assemblies. Spectrophotometric measurements were made on a Varian 2200 U.V. - Visible Spectrophotometer (Varian Co., Palo Alto, CA) fitted with jacketed cell compartment connected to external water bath and circulator Haake A81 (Haake Inc., Saddle Brooke, NJ) for temperature control at 25.0 ± 0.1 °C. Digital computer Rainbow 100 (Digital Equipment Co., Maynard MA) was used for the calculation of the stability constants through the iteration process.

F. Procedure

1. Substrate Spectral Properties

Absorption spectra of substrates were obtained to select the analytical wavelength for the determination of absorptivities. The observed values for λ_{max} and ε_{max} are summarized in table V.

Table V. Spectral Properties of sym - X—C_6H_4— C_6H_4—X

X	ε_{max} / 10^4 $M^{-1}cm^{-1}$	λ_{max} / nm
Br	2.76 [a]	262.5
COOH	3.00 [b]	283.5
CN	3.27 [a]	275.5
NO_2	2.47 [a]	311.2

a. 0.1M NaCl in 2:1 (v/v) CH_3OH: H_2O

b. 0.1M HCl in 5:1 (v/v) DMF : H_2O

2. Solubility Method.

Ligand solution preparation: Stock ligand solution was prepared by accurately weighing previously dried α-cyclodextrin, placing it in a volumetric flask, and diluting to volume with 0.1 M aqueous solution of NaCl except for 4,4' dicarboxybiphenyl, for which 0.1 M aqueous solution of HCl was used (HCl was used to repress ionization of this substrate). Further dilution of the stock solution with the diluent provided any desired concentration of the ligand.

For each substrate, an amount in considerable excess of its normal solubility was placed into each of several screw-cap sample vials with capacity of 4 dram. To each vial was added approximately 10 ml. of a desired concentration of ligand solution. Several vials without the ligand solution were prepared. For these, the dilution solvent alone was used in order to obtain the intrinsic solubility value (S_o) of the substrate. Teflon thread seal tape was placed around the mouth of each vial and the Teflon lined caps were screwed on tightly. The vials were placed in the rotating sample holder of the water bath at 25.0 ± 0.1 °C and rotated for 24 hours, by which time solubility equilibrium was reached. A portion of the supernatant solution phase was then obtained by filtration using a 0.22 micron Teflon® Filter supported by a Millipore Swag-Lok Filter Assembly. Immediately a predetermined volume was accurately withdrawn and diluted volumetrically with 0.1 M NaCl in 2:1

methanol: water; this solvent system and dilution was found to be the most appropriate for the dissociation of the complex and solubilization of the substrate, except for 4,4 dicarboxybiphenyl, in which due to solubility problems, the solvent system used was 0.1 M HCl in 5:1 N, N-dimethylformamide: water. Quantitative analysis of the total substrate was done spectrophotometrically at the λ_{max} previously determined. The length of the sample cell used was 1 cm, except for the determination of S_o for 4, 4' dibromobiphenyl, for which 10 cm cells were used because of its low solubility.

IV. RESULTS

In this chapter, experimental data from the solubility studies and the derived stability constants for α–cyclodextrin complexes with symmetrical disubstituted biphenyls as substrates in aqueous solution of 0.1 M ionic strength at 25 ± 0.1 °C are reported. Tables VI through IX contain the experimental ligand and substrate concentrations and calculated values for the variables of the linear equation 13. These tables also include the substrate intrinsic solubility, S_o, the stability constants $K_{11}$and K_{12}, and the interaction parameter a_{XX}. The estimated standard deviations are given in parentheses.

The phase solubility diagrams for disubstituted biphenyls with α–cyclodextrin are shown in figures 2, 4, 6, and 8. The curves drawn are calculated using equation 11. For this, the calculated free ligand concentration , from equation 14, was obtained by using the final estimates of the binding constants K_{11} and K_{12}. Figures 3, 5, 7, and 9 show the data plotted according to equation 13 for the calculation of the binding constants as described in the experimental part. Note that figure 8 for the dicarboxy compound only includes information for α-cyclodextrin concentrations below 0.004 M. At higher concentrations this system showed large scatter in the data and different phase solubility behavior; see figure 10 and appendix C. Furthermore, the lack of linearity in graph 9 along with the small intercept did not provide reliable K_{11}

and K_{12} values, but the analysis in the discussion part provides a quantitative description of the system.

For convenience in later discussion the results of the complex formation in this study along with results of four additional 4,4'–disubstituted biphenyls substrates studied by Andrea Paulson (47) are summarized in table X.

Table VI

Solubility data for 4,4' -Dinitrobiphenyl in 0.1 N NaCl at 25 °C

$L_t / 10^{-3}$ M	$S_t / 10^{-6}$ M	[L] $/ 10^{-3}$ M	$\frac{S_t - S_o}{[L]} / 10^{-4}$
1.2	0.95	1.19	4.05
1.2	0.98	1.19	4.35
1.6	1.29	1.59	5.19
2.0	1.49	1.99	5.13
2.0	1.69	1.99	6.15
4.0	2.99	3.99	6.32
4.0	2.94	3.99	6.20
6.0	4.90	5.99	7.39
6.0	5.01	5.99	7.59
8.0	7.11	7.98	8.32
8.0	7.65	7.98	8.99

S_o = 0.46 x 10^{-6} (0.004 x 10^{-6}) M

K_{11}= 855 (103) M^{-1}

K_{12}= 147 (17) M^{-1}

a_{xx} = 0.68 (0.11)

Table VII

Solubility data for 4,4' -Dicarbonitrilebiphenyl in 0.1 N NaCl at 25 °C

$L_t / 10^{-3}$ M	$S_t / 10^{-5}$ M	[L] $/ 10^{-3}$ M	$\frac{S_t - S_o}{[L]} / 10^{-2}$
0.4	0.58	0.39	0.18
0.4	0.58	0.39	0.18
0.8	0.62	0.79	0.15
0.8	0.60	0.79	0.13
1.2	0.67	1.19	0.13
1.2	0.67	1.19	0.13
2.0	0.89	1.99	0.19
2.0	0.85	1.99	0.17
4.0	1.26	3.99	0.18
4.0	1.27	3.99	0.19
6.0	1.79	5.98	0.21
6.0	1.74	5.98	0.20
8.0	2.22	7.97	0.21
8.0	2.33	7.97	0.22

$S_o = 0.507 \times 10^{-5}$ (0.01×10^{-5}) M

$K_{11} = 302$ (17) M^{-1}

$K_{12} = 59$ (13) M^{-1}

$a_{xx} = 0.78$ (0.18)

Table VIII

Solubility data for 4,4' -Dibromobiphenyl in 0.1 N NaCl at 25 °C

$L_t / 10^{-3}$ M	$S_t / 10^{-5}$ M	$[L] / 10^{-3}$ M	$\frac{S_t - S_o}{[L]} / 10^{-3}$
0.6	0.080	0.59	1.24
0.6	0.081	0.59	1.25
0.8	0.121	0.79	1.44
0.8	0.145	0.79	1.74
1.0	0.188	0.99	1.83
1.0	0.175	0.99	1.70
2.0	0.537	1.98	2.67
2.0	0.587	1.98	2.92
4.0	2.306	3.95	5.81
4.0	2.305	3.95	5.81
6.0	5.213	5.89	8.82
6.0	5.218	5.89	8.83
8.0	9.260	7.82	11.83
8.0	9.145	7.82	11.68
10.0	13.82	9.72	14.20
10.0	13.89	9.72	14.27

$S_o = 0.0062 \times 10^{-5} (0.002 \times 10^{-5})$ M

$K_{11} = 4332 (1445)$ M^{-1}

$K_{12} = 5335 (1562)$ M^{-1}

$a_{xx} = 4.9 (2.1)$

Table IX

Solubility data for 4,4' -Dicarboxybiphenyl in 0.1 N HCl at 25 °C

$L_t / 10^{-3}$ M	$S_t / 10^{-4}$ M	$[L] / 10^{-3}$ M	$\frac{S_t - S_o}{[L]} / 10^{-2}$
0.2	0.051	0.19	1.27
0.2	0.053	0.19	1.37
0.4	0.142	0.38	3.02
0.4	0.129	0.38	2.68
0.6	0.251	0.56	3.96
0.6	0.241	0.56	3.78
0.8	0.440	0.74	5.53
0.8	0.415	0.74	5.20
1.0	0.670	0.92	6.97
1.0	0.673	0.92	7.00
2.0	2.108	1.75	11.87
2.0	2.164	1.75	12.19
3.0	3.934	2.51	15.55
3.0	3.923	2.51	15.51
4.0	5.700	3.21	17.63
4.0	5.856	3.21	18.10

$S_o = 0.0263 \times 10^{-4}$ (0.0022×10^{-4}) M

Figure 2

Solubility of 4,4'- Dinitrobiphenyl as a function of α–Cyclodextrin concentration in aqueous solution of 0.1 M NaCl at 25 °C.

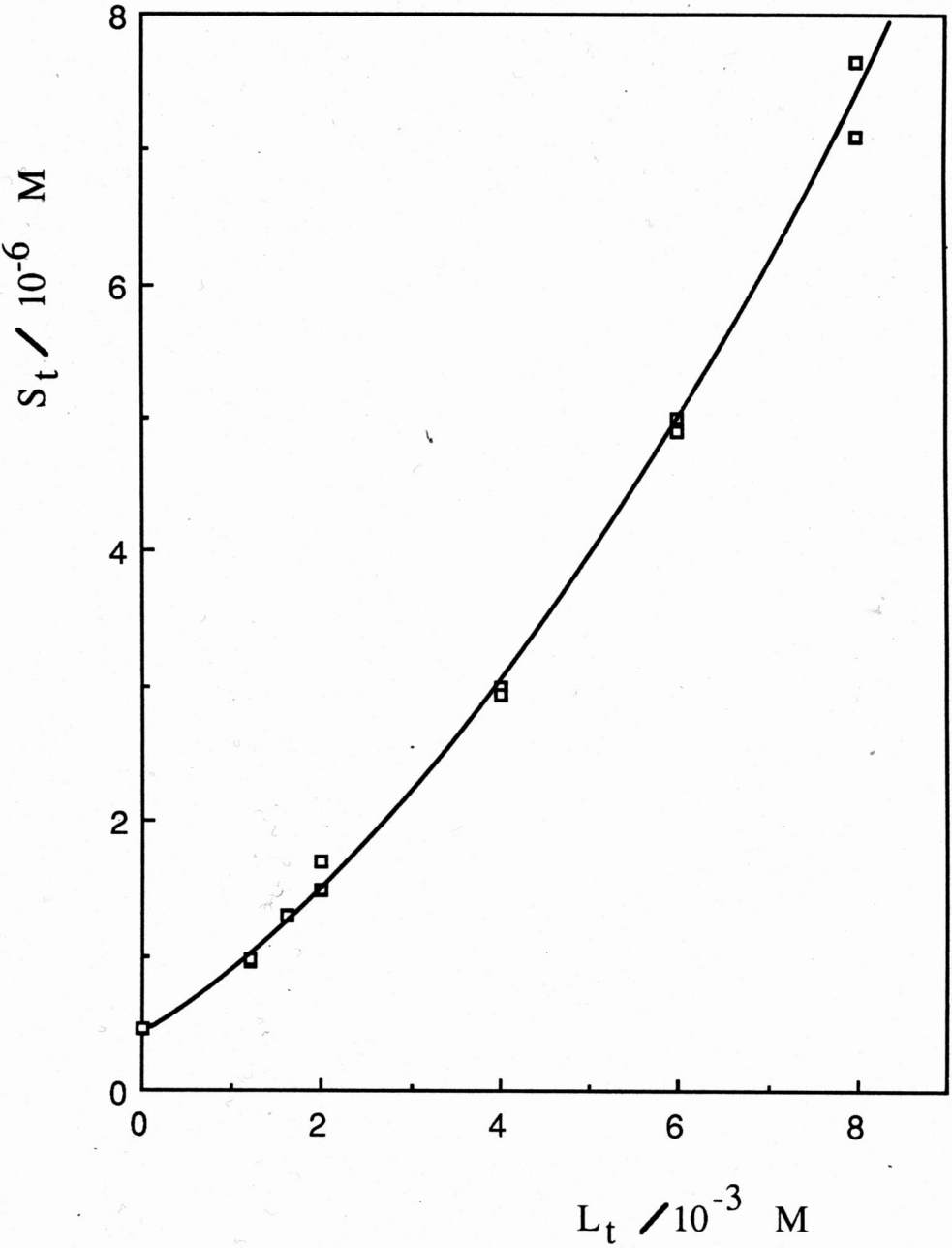
8
6
4
2
0
0
2
4
6
8
S_t / 10^{-6} M
L_t / 10^{-3} M

Figure 3

Plot of solubility data for 4,4'- Dinitrobiphenyl according to equation 13 for the determination of the binding constants K_{11} and K_{12}. Linear regression line is shown.

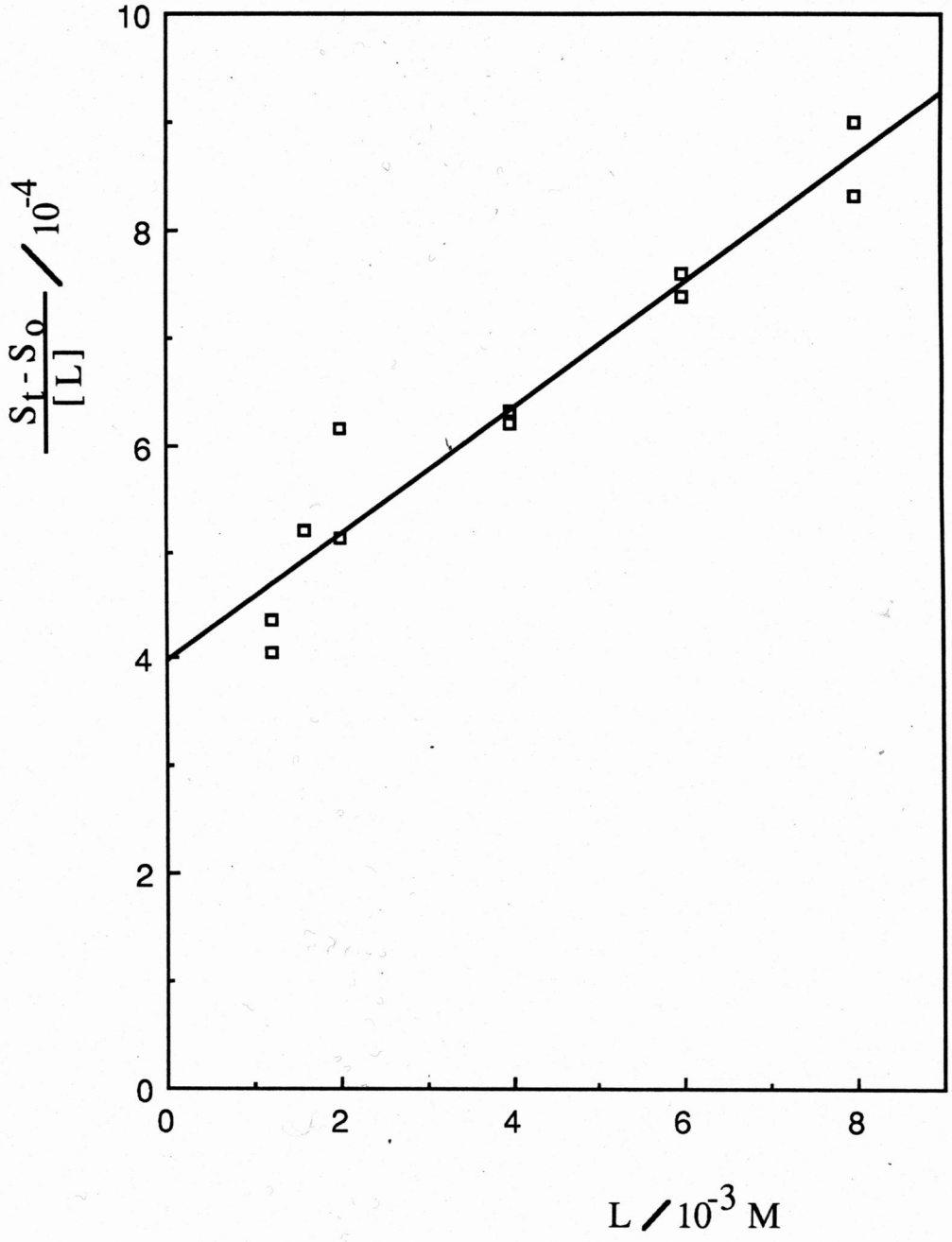
10
8
6
4
2
0
0
2
4
6
8
$\frac{S_t - S_o}{[L]} / 10^{-4}$
L / 10^{-3} M

Figure 4

Solubility of 4,4'- Dicarbonitrilebiphenyl as a function of α–Cyclodextrin concentration in aqueous solution of 0.1 M NaCl at 25 °C.

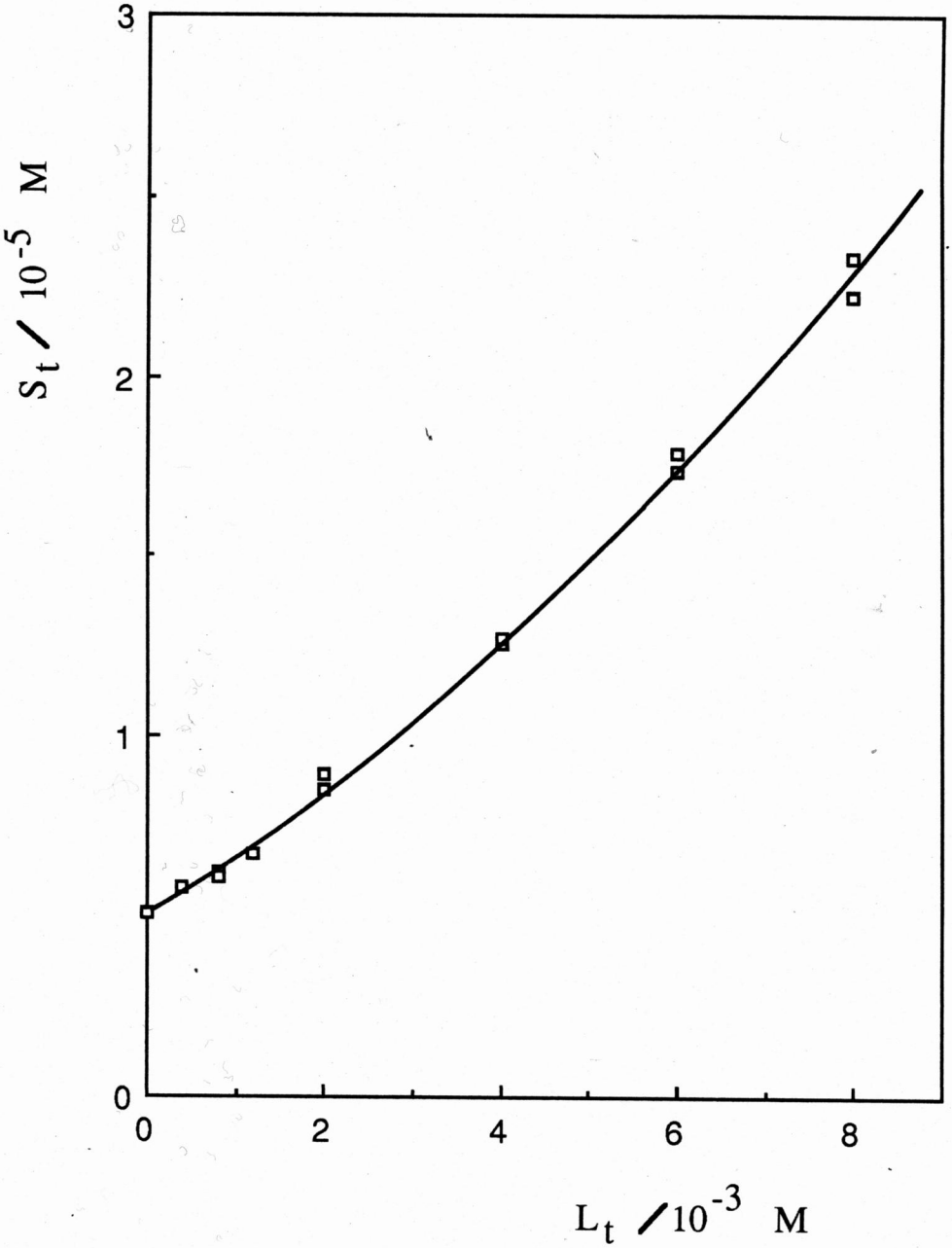
3
2
1
0
0
2
4
6
8
S_t / 10^{-5} M
L_t / 10^{-3} M

Figure 5

Plot of solubility data for 4,4'- Dicarbonitrilebiphenyl according to equation 13 for the determination of the binding constants K_{11} and K_{12}. Linear regression line is shown.

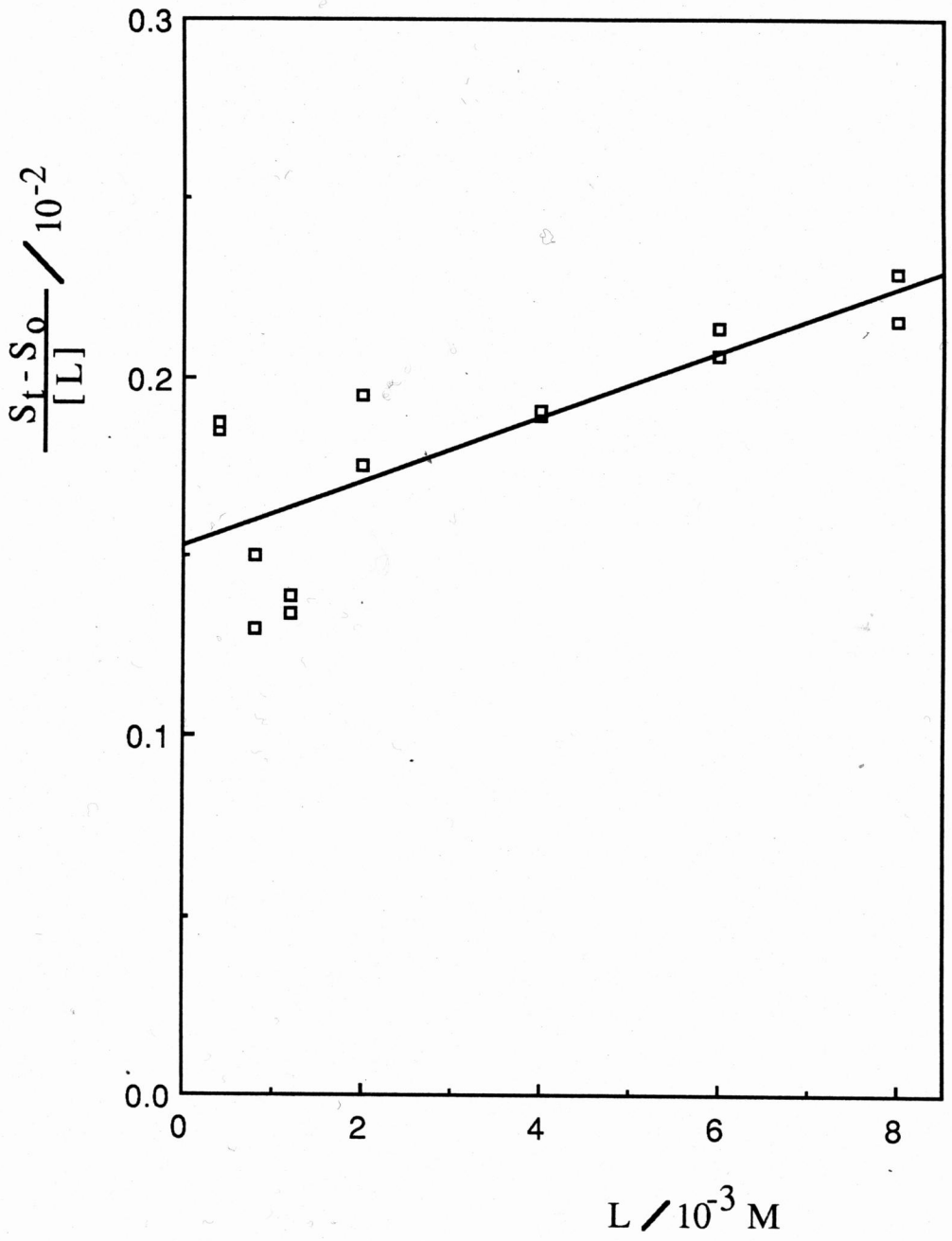
0.3
0.2
0.1
0.0
0
2
4
6
8
$\frac{S_t - S_o}{[L]} / 10^{-2}$
L / 10^{-3} M

Figure 6

Solubility of 4,4'- Dibromobiphenyl as a function of α–Cyclodextrin concentration in aqueous solution of 0.1 M NaCl at 25 °C.

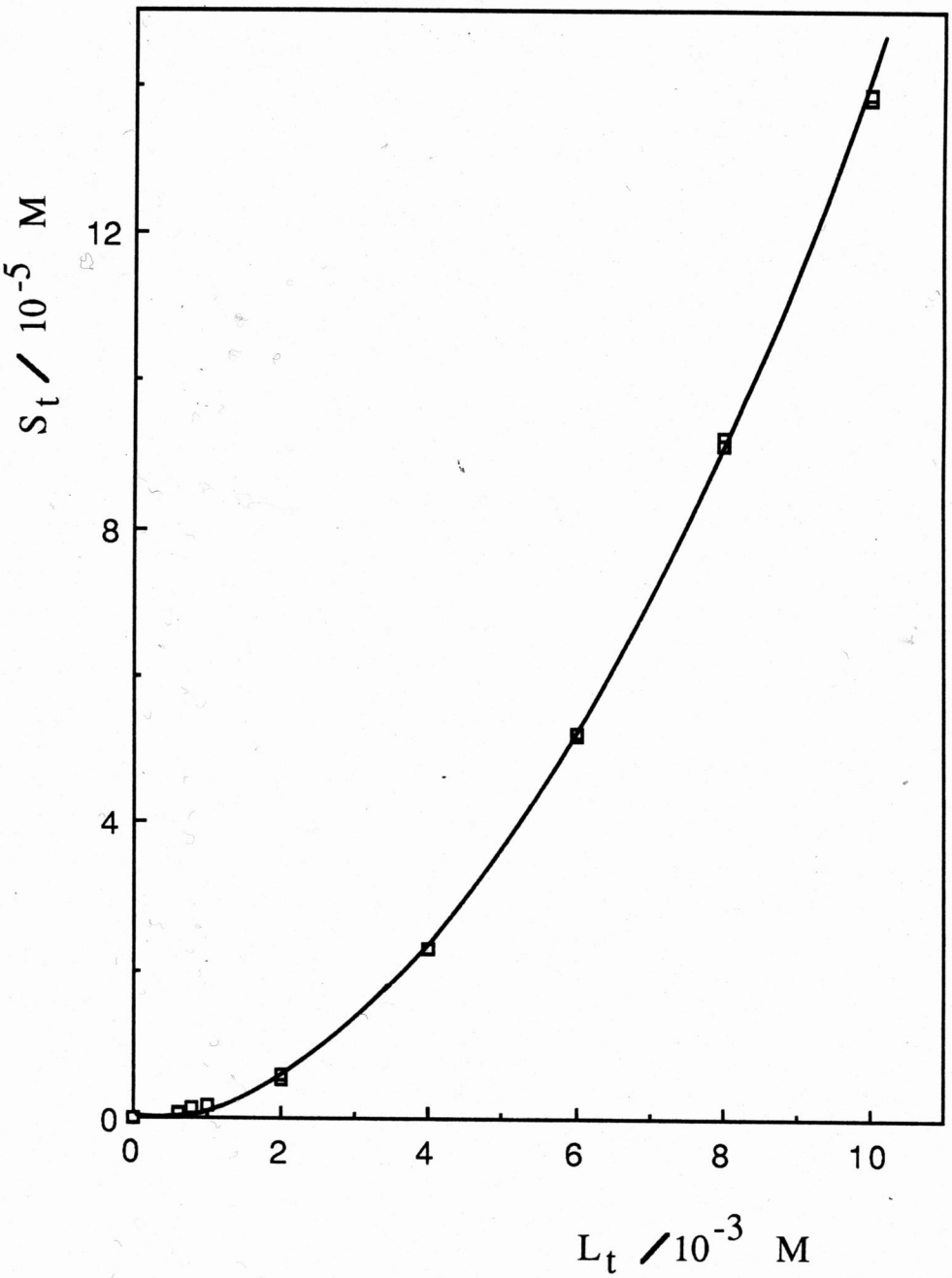
S_t / 10^{-5} M
12
8
4
0
0
2
4
6
8
10
L_t / 10^{-3} M

Figure 7

Plot of solubility data for 4,4'- Dibromobiphenyl according to equation 13 for the determination of the binding constants K_{11} and K_{12}. Linear regression line is shown.

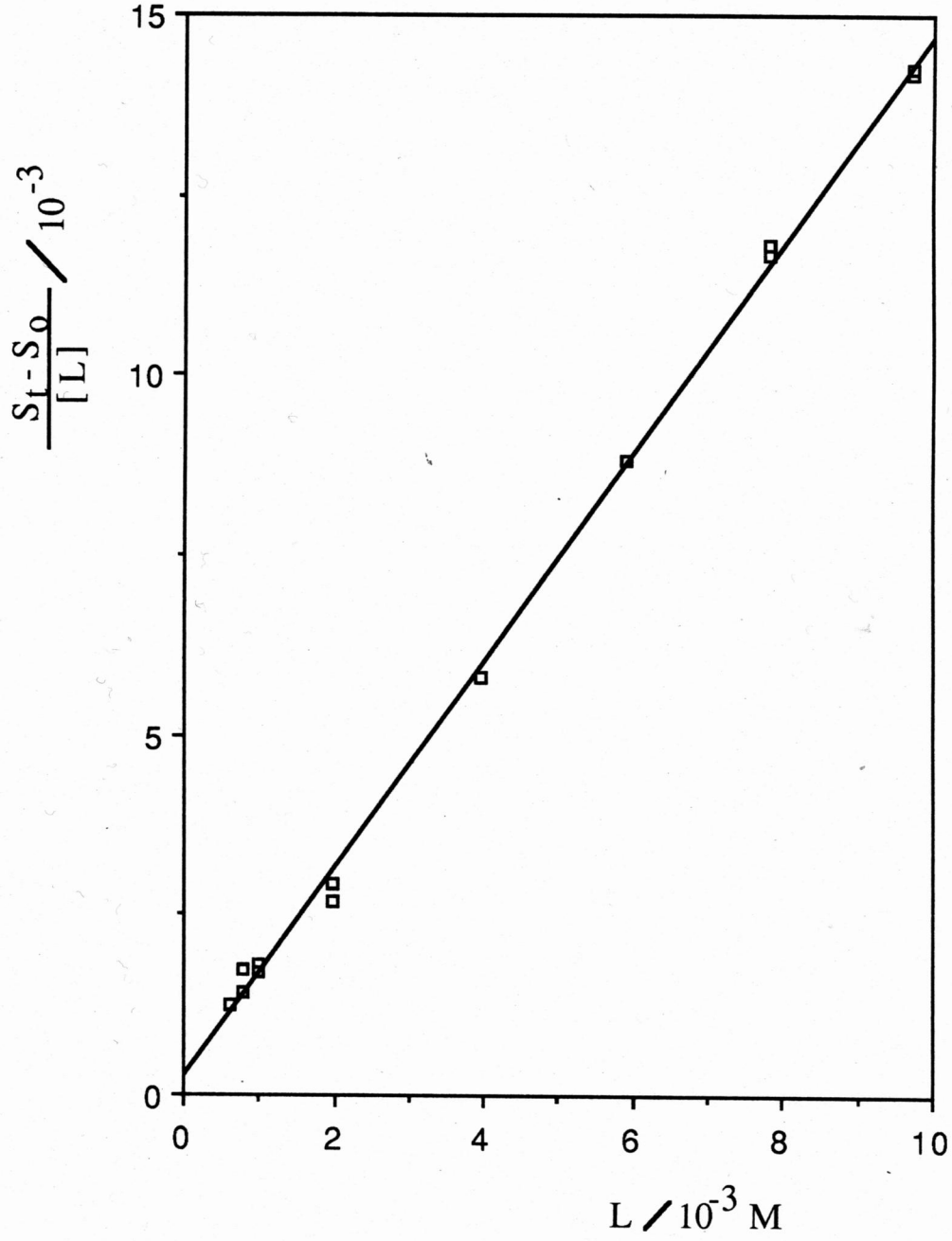
15
10
5
0
0
2
4
6
8
10
$\frac{S_t - S_0}{[L]} / 10^{-3}$
$L / 10^{-3}$ M

Figure 8

Solubility of 4,4'- Dicarboxybiphenyl as a function of α–Cyclodextrin concentration in aqueous solution of 0.1 M HCl at 25 °C.

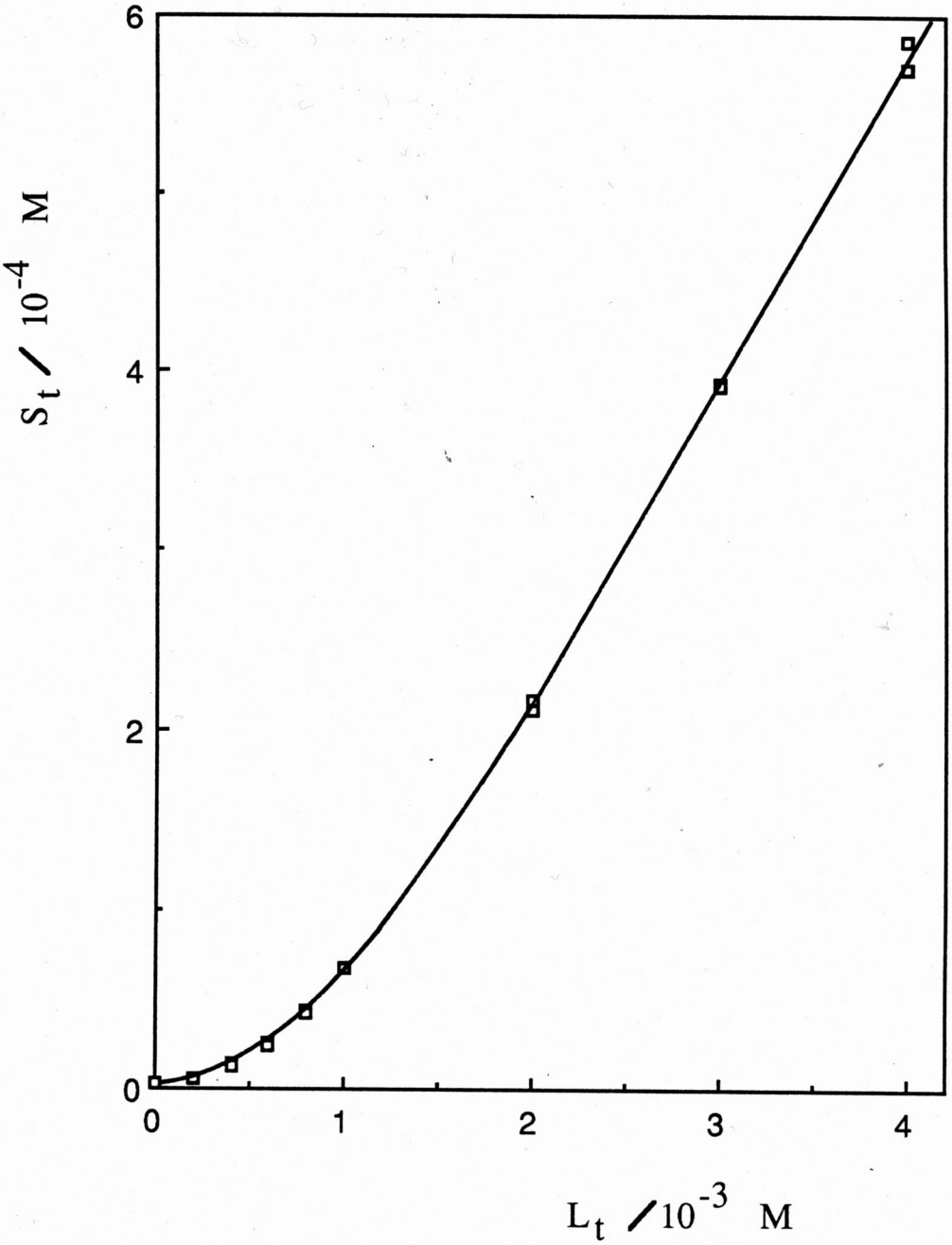
6
4
2
0
0
1
2
3
4
S_t / 10^{-4} M
L_t / 10^{-3} M

Figure 9

Plot of solubility data for 4,4'- Dicarboxybiphenyl according to equation 13 for the determination of the binding constants K_{11} and K_{12}.

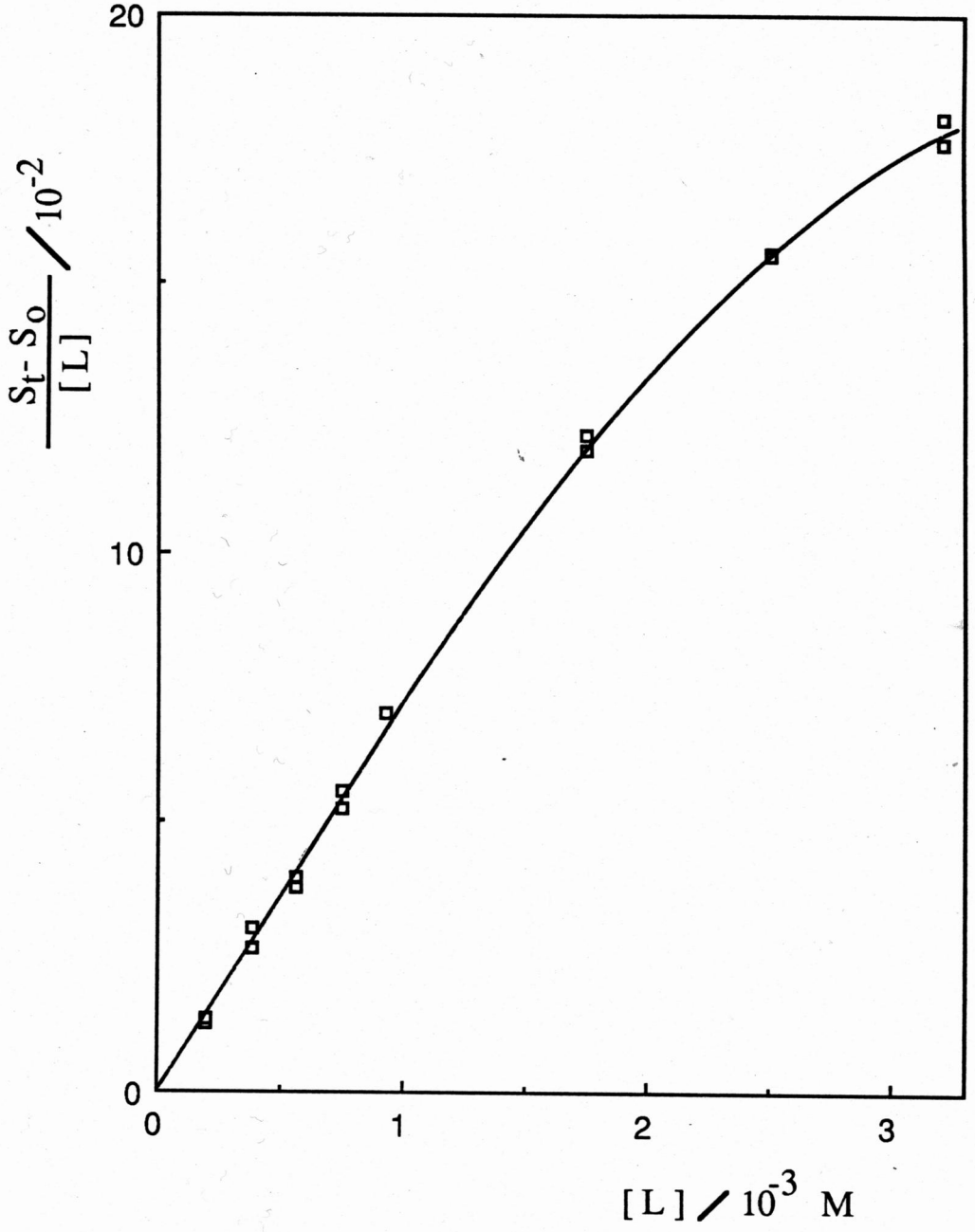
20
10
0
0
1
2
3
$\frac{S_t - S_o}{[L]} / 10^{-2}$
$[L] / 10^{-3}$ M

Table X

Stability Constants for α–Cyclodextrin complexes with sym-4,4'– Disubstituted Biphenyls, $X-C_6H_4-C_6H_4-X$, at 25 °C in 0.10 M NaCl. [a]

X	$S_o / 10^{-5}$ M	K_{11} / M^{-1}	K_{12} / M^{-1}	a_{XX}
OH [b]	19.8	41	345	33.0
	(0.1)	(5)	(48)	(6)
CH_3 [b]	0.054	1000	123	0.5
	(0.005)	(175)	(18)	(0.1)
H [b]	4.0	50	63	5.0
	(0.2)	(3)	(3)	(0.4)
Cl [b]	0.026	1030	1620	6.3
	(0.004)	(400)	(550)	(3.2)
Br	0.0062	4332	5335	4.9
	(0.002)	(1445)	(1562)	(2.1)
CN	0.507	302	59	0.78
	(0.07)	(17)	(13)	(0.18)
NO_2	0.046	855	147	0.68
	(0.004)	(103)	(17)	(0.11)
COOH [c]	0.263 [d]	-----	-----	-----
	(0.02)			

a. Standard deviation in parentheses
b. Ref. 47
c. Does not follow the binding model
d. In 0.10 M HCl

V. DISCUSSION

The substrates used in this study possess two potential binding sites. In addition, the two binding sites are identical. Thus from the binding model previously described, the stability constants are related to model parameters by

$$K_{11} = 2K_{XX}$$

$$K_{12} = \frac{a_{XX}K_{11}}{4}$$

This section is directed to the discussion of the stability constants obtained for these systems and the suitability of the substrate dissolution process as a model for binding processes.

A. Interpretation of the Solubility Diagrams

The increase in solubility of biphenyls with added α-cyclodextrin showed a positive deviation from linearity as seen in figures 2, 4, 6, and 8. The non-linear phase diagram with concave-upward curvature indicates formation of higher order complexes (37e, 38) with added α-cyclodextrin. The calculation of the individual stability constants was made by assuming that two complexes were formed, namely SL and SL_2, with the stability constants K_{11} and K_{12} given by :

$$K_{11} = \frac{[SL]}{[L][S]}$$

$$K_{12} = \frac{[SL_2]}{[SL][L]}$$

according to the binding model described by Rosanske and Connors (39). This model was confirmed when a plot of the equation 13

$$\frac{S_t - S_o}{[L]} = K_{11}S_o + K_{11}K_{12}S_o[L] \qquad \text{eq.13}$$

was shown to be linear as seen in figures 3, 5, and 7, except for 4,4'-dicarboxybiphenyl, figure 9.

Some limitations of the data treatment for the solubility method as used in this work were encountered. These difficulties were:

1. Very small value of S_o.
2. Intercept of a plot according to equation 13 is not significantly different from zero.

1. Very small value of S_o. In the 4,4'-dibromobiphenyl system the intrinsic solubility S_o could not be measured accurately due to the low substrate solubility. The total substrate solubility S_t in the presence of ligand did not present any problem for its quantification. Thus in the previous equation

$(S_t - S_o) \approx S_t$, since S_o is very small, and from the plot of this linear relationship the ratio slope/intercept will provide K_{12}; without an estimate of S_o, however, the stability constant K_{11} cannot be calculated. However, it was found that a plot of $\sqrt{S_t}$ against L_t provides a useful extrapolation estimate of the intrinsic solubility value. The plot of $\sqrt{S_t}$ against L_t for 4,4'-dibromobiphenyl, figure 10, appears to be nearly linear at low concentrations, giving the extrapolated value of $S_o = 6.25 \times 10^{-8}$M. This type of extrapolation method was done by using the lower S_t values from other disubstituted biphenyls, for which S_o was accurately known, to establish the validity of the extrapolation. A plot of extrapolated S_o against experimental S_o, figure 11, showed good agreement.

2. Intercept of a plot according to equation 13 is not significantly different from zero. The 4,4'-dicarboxylbiphenyl system does not appear to follow the model used in this study and thus the following discussion will give some interpretation to this system.

a. The plot of S_t against L_t, figure 8, is anomalous. Low L_t values display the upward curvature expected of a SL and SL_2 system, but then it becomes nearly linear.

Figure 10

Plot of $\sqrt{S_t}$ against L_t for 4,4'–dibromobiphenyl. The intercept of the linear regression line provides an extrapolated value of $S_o = 0.0062 \times 10^{-5}$ (0.002×10^{-5}) M. Standard deviation is shown in parentheses.

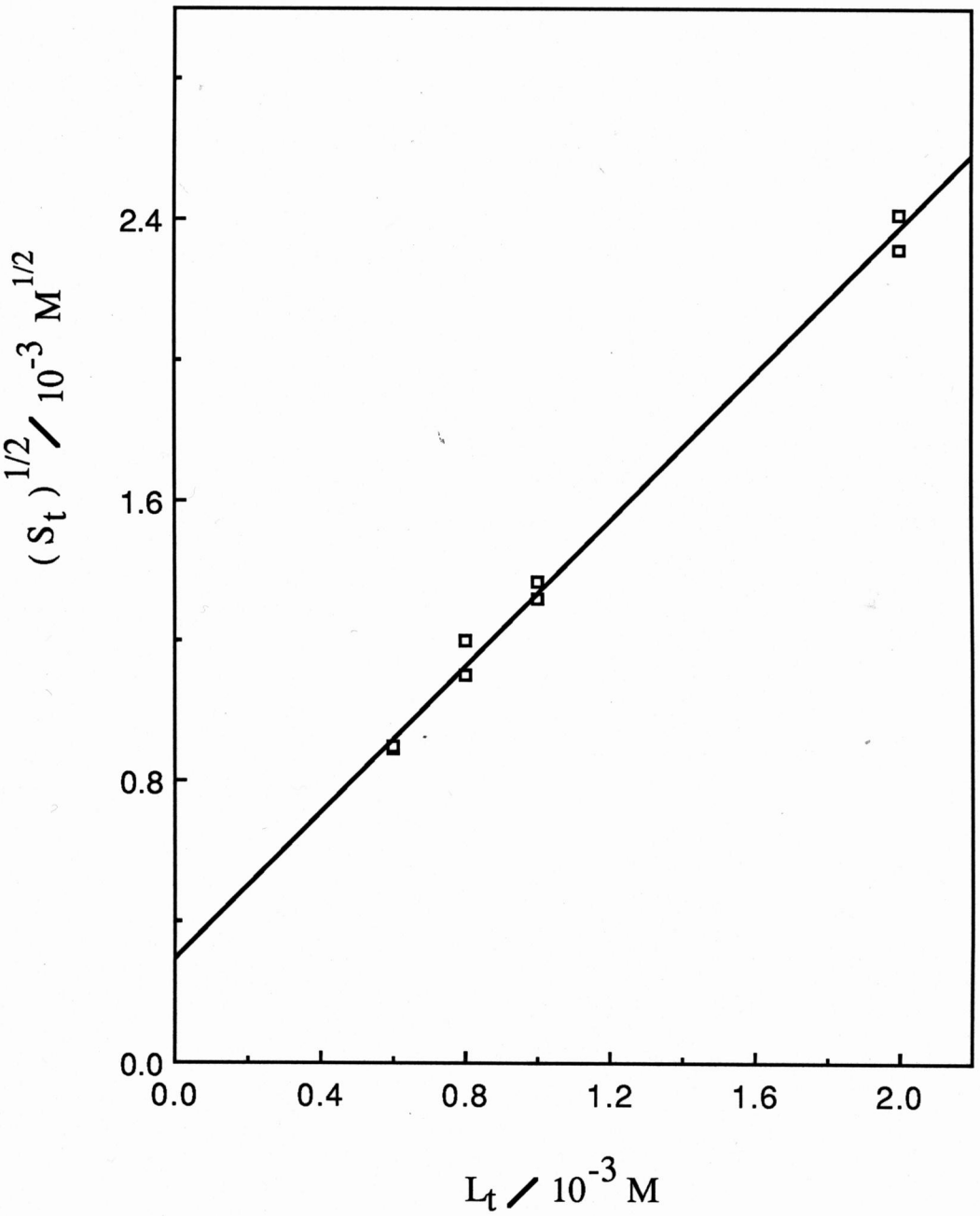
$(S_t)^{1/2} / 10^{-3}\ M^{1/2}$
2.4
1.6
0.8
0.0
0.0
0.4
0.8
1.2
1.6
2.0
$L_t / 10^{-3}\ M$

Figure 11

Plot of extrapolated $-\log S_o$ versus $-\log S_o$ experimental for six symmetrical 4,4'–disubstituted biphenyls. A line of slope one is shown for reference.

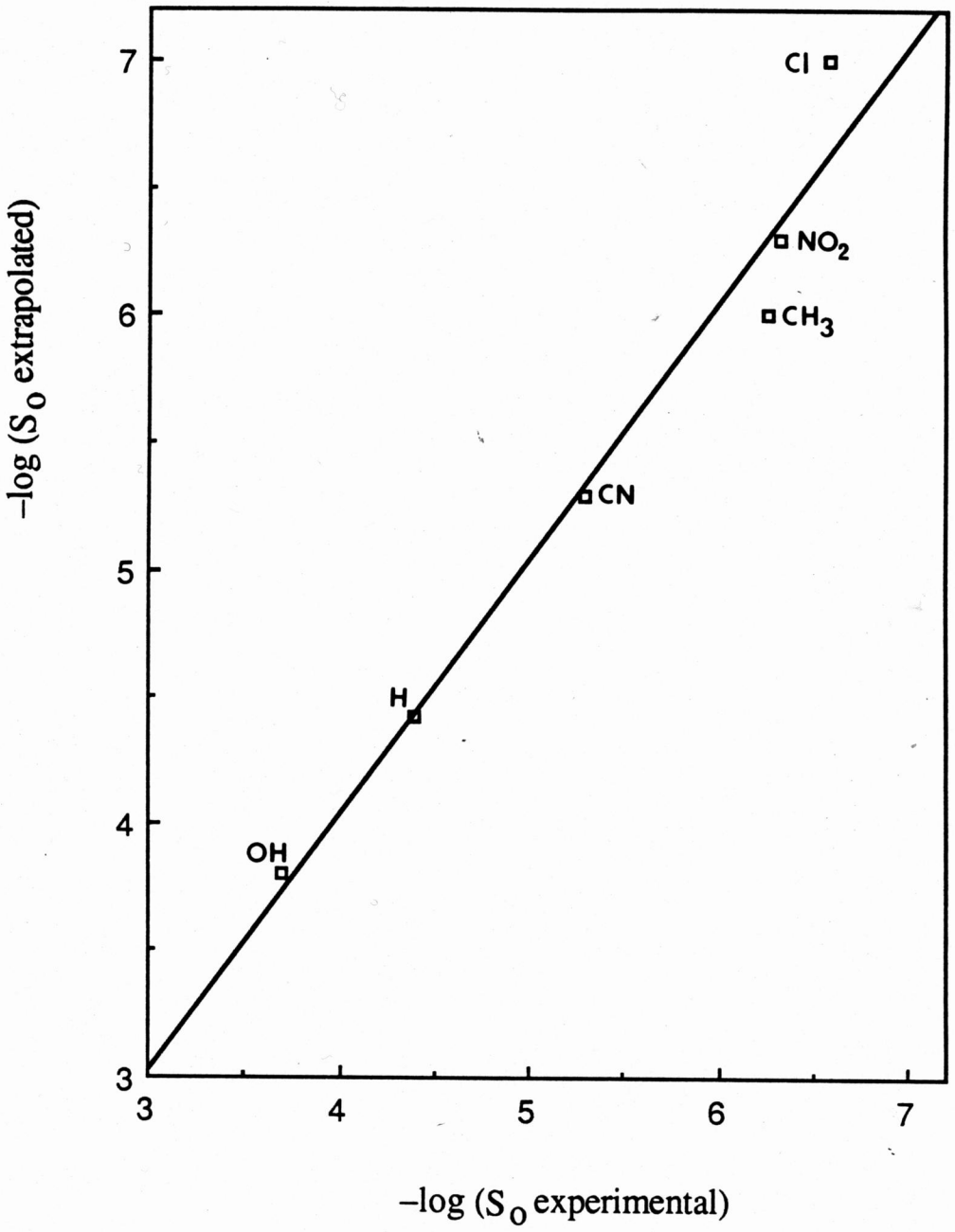
7
6
5
4
3
3
4
5
6
7
Cl
NO2
CH3
CN
H
OH
–log (S0 extrapolated)
–log (S0 experimental)

b. Analysis of the system assuming formation of SL and SL_2. In restricting our attention to ligand concentrations lower than 0.001M, the graph of equation 13 (figure 9) provides a very small intercept (less than 0.002) and the slope = $K_{11}K_{12}S_o = 76\ M^{-1}$. Because of the uncertainty of the intercept the binding constants cannot be obtained individually. However, since $S_o = 2.63 \times 10^{-6}M$

then $\beta_{12} = K_{11}K_{12} = 2.8 \times 10^7$.

c. Evaluation of a possible stoichiometry. A graphical technique can be used for the determination of reasonable stoichiometric ratios (37). The overall formation of a complex SL_n can be written as

$$S + nL \rightleftharpoons SL_n$$

and the overall stability contact is given by

$$\beta_{1n} = \frac{[SL_n]}{[S][L]^n}$$

rearranging, taking logarithms, and since $[S] = S_o$ and $[SL_2] = S_t - S_o$, equation 20 is obtained.

$$\log\left(\frac{S_t - S_o}{S_o}\right) = \log \beta_{1n} + n \log [L] \qquad \text{eq.20}$$

A plot of log [$(S_t - S_o) / S_o$] against log [L] according to equation 20 will give a straight line for the system with slope equal to the stoichiometric coefficient n. The preliminary analysis was done by assuming [L] = L_t. Subsequently the first estimate of β_{12} was used to calculate [L] from equation 21. Figure 12 shows the log - log plot according to equation 20, giving the stoichiometric coefficient n = 2, indicating formation of SL_2. Therefore, it is possible to assume the following binding process

$$S + 2L \rightleftharpoons SL_2$$

$$\beta_{12} = \frac{[SL_2]}{[S][L]^2} \qquad \text{eq.21}$$

thus the mass balance equation for the substrate is given by equation 22

$$S_t = S_o + \beta_{12} S_o [L]^2 \qquad \text{eq. 22}$$

A plot of S_t against $[L]^2$ will give a straight line with slope equal to $\beta_{12}S_o$.

Figure 13 depicts the system according to equation 22, giving $\beta_{12}S_o = 76\ M^{-1}$

Figure 12

Plot of log [$(S_t - S_o) / S_o$] against log [L] for 4,4'–dicarboxylbiphenyl according to equation 20. The equation of the line is given by:

$$\log [(S_t - S_o) / S_o] = 7.457 + 1.99 \log [L]$$

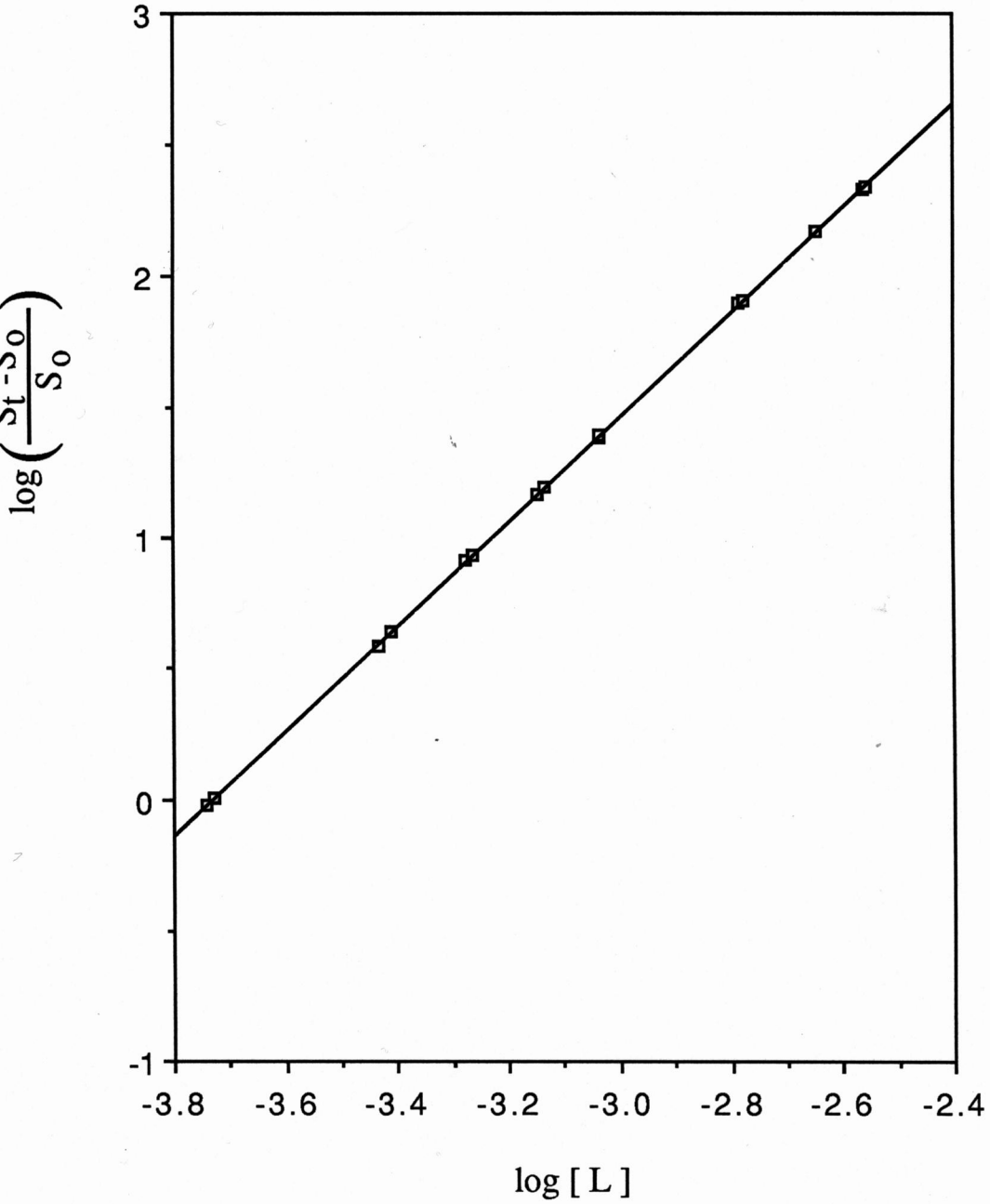
3
2
1
0
-1
-3.8
-3.6
-3.4
-3.2
-3.0
-2.8
-2.6
-2.4
log [L]
log (St - So / So)

Figure 13

Plot of S_t versus $[L]^2$ for 4,4'–dicarboxylbiphenyl according to equation 22. The intercept and the slope provide the intrinsic solubility $S_o = 2.61 \times 10^{-6}$ M and $\beta = 2.9 \times 10^7$ M^{-2}, respectively. The linear regression line is shown.

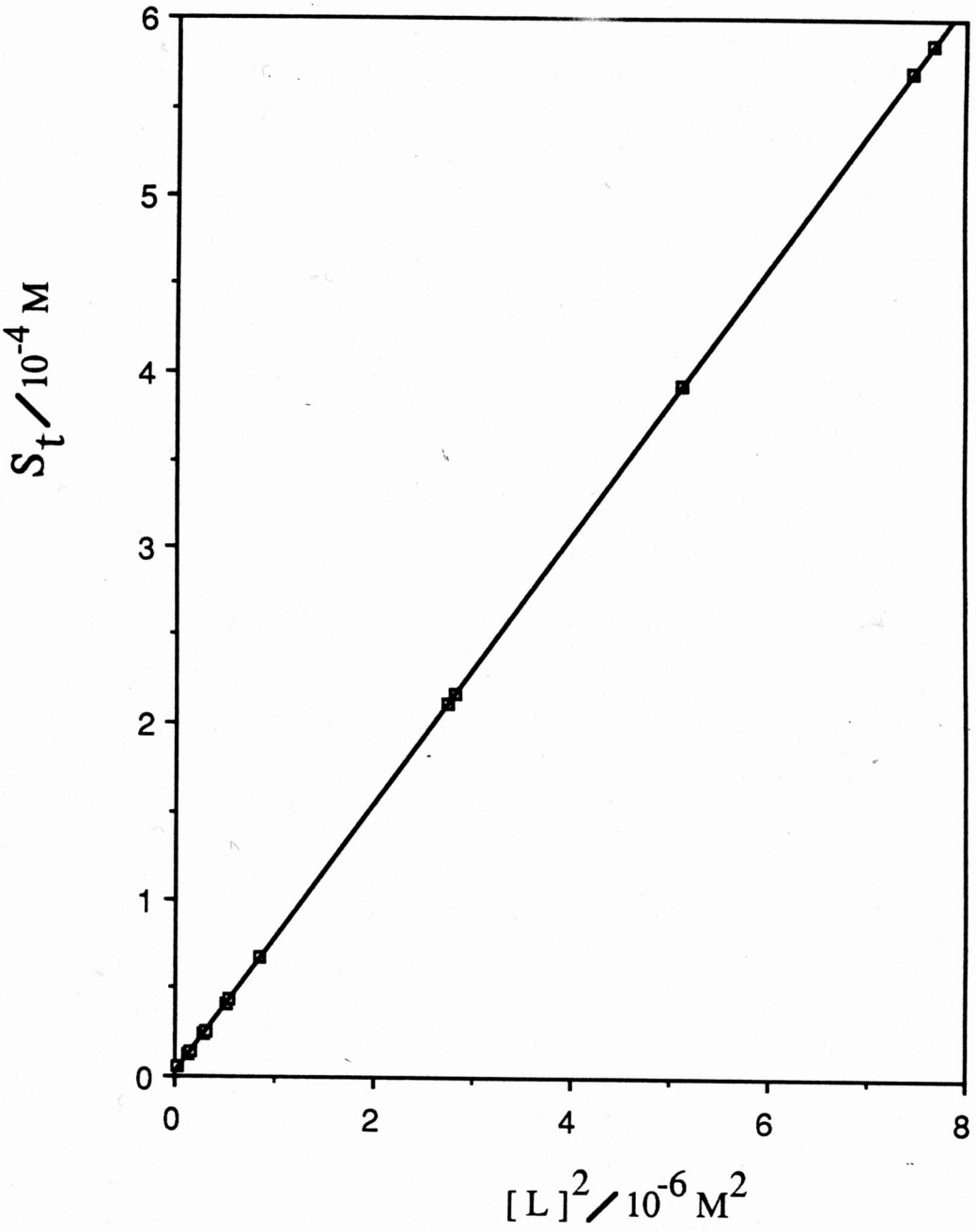
6
5
4
3
2
1
0
0
2
4
6
8
$S_t / 10^{-4}$ M
$[L]^2 / 10^{-6}$ M^2

and $S_o = 2.61 \times 10^{-6}$ M. Therefore, $K_{11}K_{12} = 2.9 \times 10^7$ M^{-2}, which is in good agreement with the estimate obtained earlier.

From the previous analysis, it is possible to treat the data (below $L_t = 0.004$ M) according to the cooperative system $K_{12}>>>K_{11}$, so no SL is detectable and the detectable complex is present as SL_2, with

$\beta_{12} = K_{11}K_{12} = 2.9 \times 10^7$ M^{-2}.

B. Discussion of the Binding Constant

The binding constants K_{11} and K_{12} are empirical parameters that reflect, in general, a competition among medium - medium, medium - solute, and all solute - solute interactions. Connors and Pendergast (41) proposed a model that accounts for these interactions by means of the following equation:

$$\Delta G^\circ_{X'X} = \Delta G^\circ_{MM} + \Delta G^\circ_{MS} + \Delta G^\circ_{SS}$$

where $\Delta G^\circ_{X'X} = -RT \ln K_{X'X}$ and $K_{X'X}$ is the microscopic binding constant for the binding to site X. The free energy changes due to medium - medium, medium - solute, and solute - solute interactions are given by the free energy terms ΔG°_{MM}, ΔG°_{MS} and ΔG°_{SS}, respectively.

Medium - medium interactions include the solvophobic effect. The association of two solute molecules will depend on the solvent and substrate

polarity compared to that of the interior of the cyclodextrin. In the case of a polar solvent the association of a non-polar substrate and ligand is due to the molecules' tendency to reduce the area of solute-solvent interphase, resulting in a reduction of the free energy.

Medium - solute interaction represents all solvation phenomena. The role of this interaction may be stabilizing or destabilizing depending on the polarity of the substrate binding site. Strictly speaking, the $\Delta G°_{MS}$ contains contributions of all three species (solvent, ligand, and substrate); it is not possible to ascribe the increase or decrease in energy of the system just to change in the solvation of one specie. However, non-polar substrate solvation will be reduced upon complexation. Therefore, the decrease in solvation of the substrate decreases the energy of the system.

Solute-solute interactions include interactions between the ligand and binding site in the 1:1 and 1:2 complexes, substrate-substrate interaction, and possibly ligand-ligand interaction in the 1:2 complex. The main contributions to the $\Delta G°_{SS}$ are the electrostatic, induction and dispersion forces, and hydrogen bonding. The magnitude of these forces is affected by the site electron density and polarizability.

From what has been described in this section, in comparing two complexes and deciding what makes one complex more stable than another, one is confronted with the fact that none of the factors previously described is

overwhelming in deciding stabilities. The concept described, mainly that complex stability is determined by polarity, polarizability, and binding site electron density, will be used in describing the biphenyl system.

In viewing the biphenyl system the hydrophobic contribution can only favor the complex formation since the solvent used, water, is more polar than the interior of the cyclodextrin and the substrates are non-polar compounds. Polarizability and binding site election may or may not favor the complex formation.

1. Binding Constant K_{11}

Weak interactions were found with OH and H substituents compared to all other electron-attracting substituents. For the latter substituents, there is a relatively high electron density at the X binding site by the electron-withdrawing inductive effect, and they are extremely polarizable. Increase in substrate site polarizability was postulated (40, 43, 44) to be complex stabilizing. Therefore, the binding constants K_{11} are high. Anomalously large K_{11} value was observed with the dimethyl substituted compound. This compound was not studied in the benzene series (42). However, this substituent has been shown to be anomalous in other studies. Wong, Lin, and Connors (44) studied the complexation of α-cyclodextrin and a series of 4-substituted anilines at 25°. The K_{11} values obtained for the complexation of the conjugate base form of the aniline are given in Table XI. The substituents are ordered in terms of their

Table XI

Stability Constants for α-Cyclodextrin complexes with 4-Substituted anilines, $X - C_6H_4 - NH_2$, at 25 °C. [a]

X	K_{11} / M^{-1}
NH_2	2.6
OCH_3	6.7
CH_3	57.6
H	8.8
COO^- [b]	9.0
Cl	251.0
COOH[b]	1341.0
CN	451.0
NO_2	635.0

a. Ref. 44
b. Ref. 40

increasing Hammett substituent parameter value. By comparing the rank order in this series, it is possible to observe that the 4-methylaniline is anomalously large. Note that also the 4-aminobenzoic acid presents some deviation.

2. Binding Constant K_{12}

The stability constants K_{12} compared to the K_{11} values showed three relationships (See Table X):

a. $K_{12} < K_{11}$ (mainly for the electron-withdrawing substituents)

b. $K_{12} > K_{11}$ (mainly for the electron-donating substituents)

c. $K_{12} \approx K_{11}$ (considering the standard deviations)

These changes have been observed in other systems (40, 42, 43, 44). The electronic distribution for a symmetrical disubstituted compound was previously described as a hybrid of resonance forms (see scheme III) Thus if substituent X is electron-withdrawing (resonance form 3) the ligand can act as a sink for electrons. This effect produces a partial charge transfer from the X' site to the ligand in the X'X and then from X site due to the resonance. Thus the X site in X'X is less electron rich than the X site in XX. Decrease in substrate site electron density was postulated to decrease the complex stability (40, 43, 44). Therefore, the binding constant K_{12} decreases. For the

electron-donating substituents the opposite drift of charge takes place, and the K_{12} values are increased. In the cases where K_{12} was about the same (Cl and Br) , it will be necessary to understand the existence of ligang-ligand interactions. These effects were considered by Connors and Pendergast (41) in the anlaysis of the interaction parameter a_{XX}. The effects on the magnitude of a_{XX} were divided into the following three classes.

i). The electronic effect: This concept was previously discussed.

ii). The repositioning effect: When a 1:1 complex has been formed, the substrate and ligand acquire a relative position that minimizes the total free energy of the system. The formation of the 1:2 complex will also tend to minimize the total free energy. The optimization of the 1:2 complex may require modification of the original position of the molecules in the 1:1 complex. Such repositioning will mean that the 1:2 complex be less stable.

iii). The ligand-ligand interaction effect: In the 1:2 complex attractive interactions may exist between the facing rims of the two cyclodextrins. Any repulsive interaction will be part of the repositioning effect. Therefore, the ligand-ligand interaction effect is 1:2 complex stabilizing.

From the aforementioned effects, it will be possible to understand why

even though Br and Cl are electron-withdrawing substituents their stability constants K_{12} did not decrease as expected due to the possibility of a larger influence of the ligand-ligand interaction effect.

C. Binding Process and the Substrate Dissolution

The possibility that the binding process is related to the solubility of a substrate has its basis in the competition between solute-solute and solute-solvent interactions (38). As a rough generalization among systems similar to the type used in this work, the extent of complex formation should be inversely related to reactant solubility (38,41). In this section the correlation between substrate dissolution process and the possible binding processes, based on the context of symmetrical disubstituted substrates, are examined. Table XII shows the different binding processes along with the model (solubility) process and the graph that may suggest the existence of such correlation.

Figure 14 depicts the first binding process. For all the 4,4' disubstituted biphenyls a good linear relationship was observed. The equation of the line is

$$\log K_{11} = -0.578\ (0.045)\ \log S_o - 0.66\ (0.26)$$

Standard deviations of the slope and intercept are shown in parentheses.

For all other binding processes there were no useful correlations. The lack of correlation is not greatly surprising since the model process does not

Table XII

Substrate Solubility Model and Binding Processes

Binding Process	Model process	Graph
$S + L \overset{K_{11}}{\rightleftharpoons} SL$	$S\,(sat.) \overset{1/S_o}{\rightleftharpoons} S\,(solid)$	$\log K_{11}$ vs $-\log S_o$
$SL + L \overset{K_{12}}{\rightleftharpoons} SL_2$	$S\,(sat.) \overset{1/S_o}{\rightleftharpoons} S\,(solid)$	$\log K_{12}$ vs $-\log S_o$
$S + 2L \overset{\beta_{12}}{\rightleftharpoons} SL_2$ $\beta_{12} = K_{11}K_{12}$	$S\,(sat.) \overset{1/S_o}{\rightleftharpoons} S\,(solid)$	$\log \beta_{12}$ vs $-\log S_o$
$2SL \overset{a_{XX}/4}{\rightleftharpoons} SL_2 + S$	$S\,(sat.) \overset{1/S_o}{\rightleftharpoons} S\,(solid)$	$\log a_{XX}$ vs $-\log S_o$

Figure 14

Plot of log K_{11} versus –log S_o for seven symmetrical 4,4'–disubstituted biphenyls. The straight line was computed using linear regression. the equation of the line is

$$\log K_{11} = -0.578\ (0.045) \log S_o - 0.66\ (0.26) \qquad r = 0.99$$

Standard deviation of the slope and intercept are shown in parentheses.

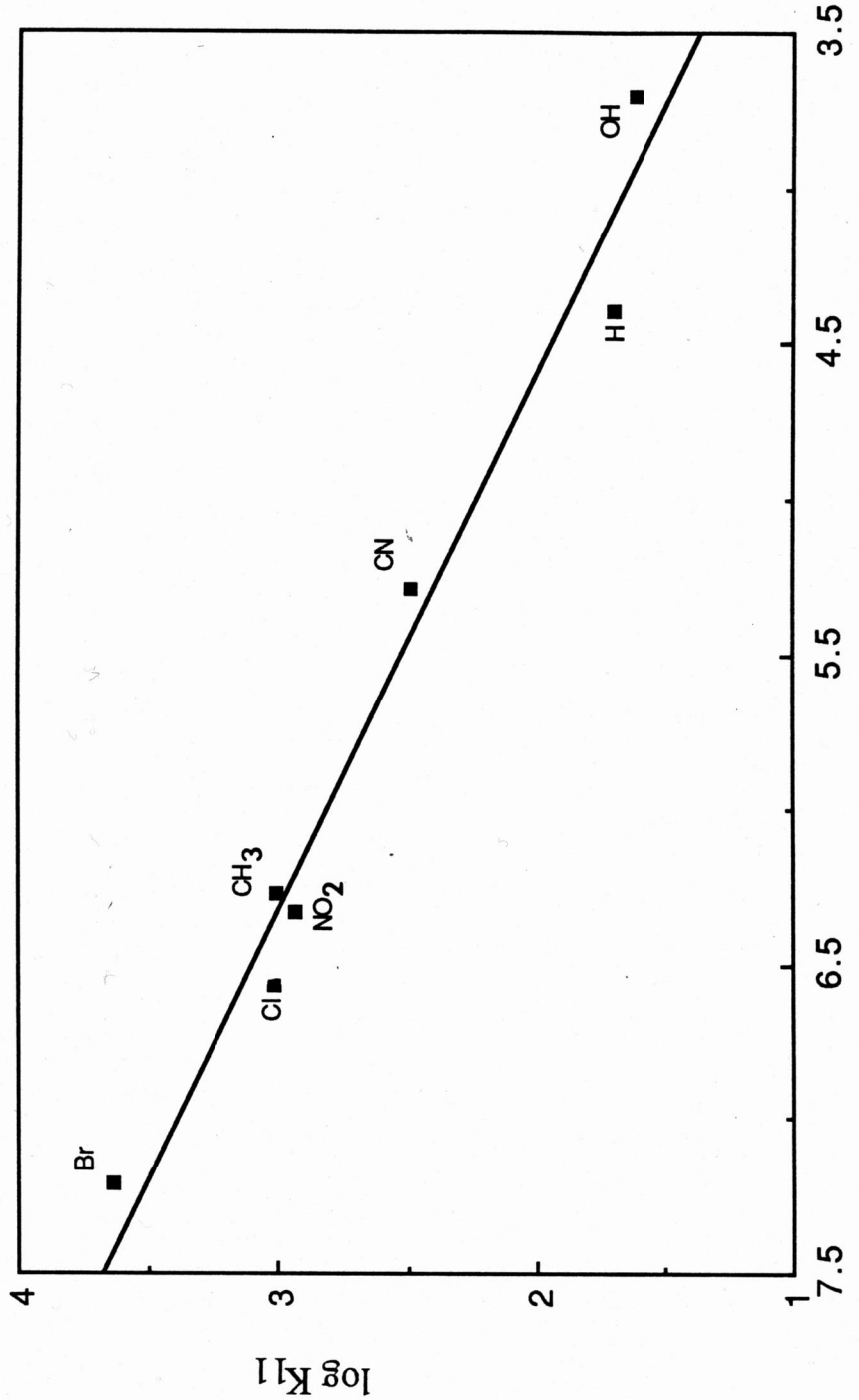
log K1 1
4
3
2
1
7.5
6.5
5.5
4.5
3.5
−log S0
Br
Cl
CH3
NO2
CN
H
OH

include any ligand-ligand interaction effect. Any binding process that includes 1:2 binding may bring in the electronic, re-positioning, and ligand-ligand interaction effects.

D. Comparison of the Relationship between K_{11} and S_o for the Benzene and Biphenyl series.

Pendergast found an inverse relationship between K_{11} and S_o. A good linear correlation was observed for most of the ten substituents, the equation of the line being:

$$\log K_{11} = -0.59 \log S_o + 0.40$$

The relationship between K_{11} and S_o for the biphenyl series is given by the following equation

$$\log K_{11} = -0.578 \log S_o - 0.66$$

The slopes of these equations are not significantly different at 95% confidence level . Figure 15 shows the relationship between the binding constant K_{11} and the intrinsic solubility S_o for both series plotted in the same graph. The previous relationship for both series is an indication of a similarity between the solubility model and the binding process, which does not include K_{12} binding, for the biphenyl and benzene series.

Figure 15

Plot of log K_{11} against $-\log S_o$ for

$X - C_6H_4 - X$, open squares (41)

$X - C_6H_4 - C_6H_4 - X$, closed squares

Linear regression lines shown (note that NO_2, CN,and COMe were not used for the linear regression of the benzene series)

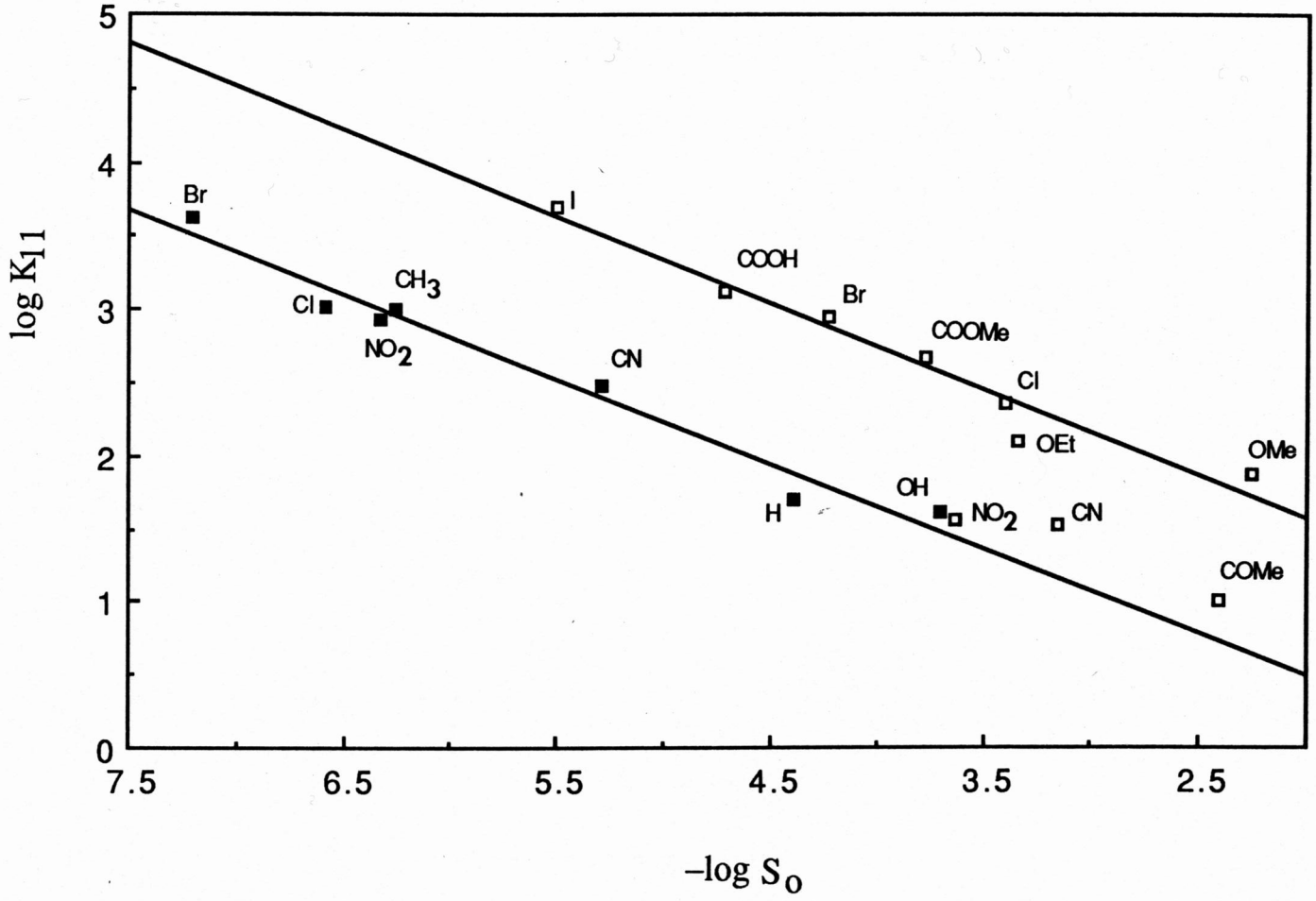
log K_{11}
5
4
3
2
1
0
7.5
6.5
5.5
4.5
3.5
2.5
–log S_o
Br
Cl
CH_3
NO_2
CN
H
OH
NO_2
CN
I
COOH
Br
COOMe
Cl
OEt
OMe
COMe

E. Summary

Complex formation of α-cyclodextrin and 4,4'-disubstituted biphenyls was studied by determining the experimental stability constants. The substrates used in this study possess two identical binding sites. The calculation of the stability constants was made by assuming that two complexes were formed, namely SL and SL_2, with stability constants K_{11} and K_{12}. Some limitations of the data treatment used in this work were encountered. First, the 4,4'-dibromobiphenyl substrate intrinsic solubility S_o was too small to be measured accurately. However it was found that a plot of $\sqrt{S_t}$ against L_t provides a useful extrapolation estimate. For 4,4'-dibromobiphenyl in 0.1 M NaCl aqueous solution $S_o = 6.2 \times 10^{-8}$ M. Second, all the substrates except the 4,4'-dicarboxylbiphenyl followed the binding model assumed. The latter substrate was found to follow a model where $K_{12} >>> K_{11}$ so no SL is detectable and the detectable complex is present as SL_2, with $\beta_{12} = K_{11}K_{12} = 2.9 \times 10^7\ M^{-2}$.

The correlation between substrate dissolution process and the possible binding process, based on the context of symmetrical disubstituted substrates, was examined. A good correlation was observed when the model

slopes of the equation that relates K_{11} and S_o in the benzene and biphenyl series were not significantly different at 95 % confidence level. This correlation is an indication of a similarity between solubility model and the binding process for the biphenyl and benzene series.

VI. REFERENCES

1. A. Villiers, *Compt. Rend.*, *112*, 536 (1891)
2. F. Schardinger, *Wien. Klin. Wochenschr.*, *17*, 207 (1904)
3. M.L. Bender, R.L. Van Etten, G. A. Clowes, and J. F. Sebastian , *J. Am. Chem. Soc.*, *88*, 2318 (1966)
4. J. Szejtli in "Inclusion Compounds", Eds. J. L. Atwood, J. E. D. Davies, D. D. MacNicol., Academic Press Inc., London, vol. 3, 331-390 (1984)
5. D. French, *Adv. Carbohydrate Chem.*, *12*, 189 (1957)
6. M. L. Bender and M. Komiyama, "Cyclodextrin Chemistry" Springer-Verlag, Berling (1978)
7. J. A. Thoma and L. Stewart in "Starch Chemistry and Technology", vol. I, R. L. Whistler and E. F. Paschall, Eds. Academic, New York, N. Y. 209-249 (1965)
8. M. Yamamoto and K. Horikoshi, *Starch / Starke*, *33*, 244 (1981)
9. W. Saenger, *Angew. Chem. Itern. Ed.*, *19*, 344 (1980)
10. J. Szejtli, "Cyclodextrin and their Inclusion Complexes" Akademiai Kiado; Budapest, D. Reidel Publishing Co., Dordrecht, Holland (1982)
11. P. R. Sundarajan and V. S. R. Rao, *Carbohydr. Res.*, *13*, 351 (1970)
12. V. G.Murphy, B.Zaslow and A. D.French, *Biopolymers*, *14*, 1487 (1975)
13. V. S. R. Rao and J. F. Foster, *J. Phys. Chem.*, *67*, 951 (1963)
14. C. A. Glass, *Can. J. Chem.*, *43*, 2652 (1965)
15. K. Takeo and T. kuge, *Agr. Biol. Chem.*, *34*, 1416 (1970)

16. A. Hybl, R. E. Rundle, and D. E. Williams, *J. Amer. Chem. Soc.*, *87*, 2779 (1965)

17. R. Bergeron and M.A. Channing, *Bioorg. Chem.*, *5*, 437 (1976)

18. B. Casu, M. Reggiani, G. G. Gallo, and A. Vigevani, *Tetrahedron*, *22*, 3061 (1966)

19. D. French, M. L. Levine, J. H. Pazur, and E. Norberg, *J. Amer. Chem. Soc.*, *71*, 353 (1949)

20. M. J. Jozwiakowski and K. A. Connors, *Carbohydr. Res.*, *143*, 51 (1985)

21. W. J. James, D. French, and R. E. Rundle, *Acta Cryst.*, *12*, 385 (1959)

22. F. Cramer, *Revs. Pure Appl. Chem.*, *5*, 143 (1955)

23. W. Saenger, *Agnew. Chem. Int. Ed. Eng.*, *19*, 344 (1980)

24. N. Wiedenhof and J. N. J. Lammers, *Carbohydr. Res.*, *7*, 1 (1968)

25. P. C. Manor and W. Saenger, *J. Amer. Chem. Soc.*, *96*, 3630 (1974)

26. K. K. Chacko and W. Saenger, *J. Amer. Chem. Soc.*, *103*, 1708 (1981)

27. W. Saenger, M Noltemeyer, P. C. Manor, B. Hingerty, and B. Klar, *Bioorg. Chem.*, *5*, 187 (1976)

28. R. J. Bergeron in "Inclusion Compounds", Eds. J. L. Atwood, J. E. Davies, D.D. MacNicol, Academic Press Inc., London, vol. 3, 394 (1984)

29. I. Tabushi and L. C. Yuan , *J. Amer. Chem. Soc.*, *103*, 3574 (1981)

30. J.A. Hamilto, L. K. Steinrauf, and R. L. Van Etten, *Acta Cryst.*, *B24*, 1560, (1968)

31. P. V. Demarco and A. L. Thakkar, *J. Chem. Soc., Chem. Commun.*, 2, (1970)

32. D. J. Wood, F. E. Hruska, and W. Saenger, *J. Amer. Chem. Soc.*, *99*, 1735 (1977)

33. K. Harata, *Bull. Chem. Soc. Jpn.*, *50*, 1416 (1977)

34. M. Komiyama and H. Hirai, *Bull. Chem. Soc. Jpn.*, *54*, 828 (1981)

35. R. I. Gelb, L. M. Schwartz, M. Radeos, R. B. Edmonds, and D. A. Laufer, *J. Amer. Chem. Soc.*, *104*, 6283 (1982)

36. (a) D. W. Griffiths and M. L. Bender, "Advances in Catalysis", Eds. D. D. Eley, H. Pines, and P. B. Weisz, Academic Press, New York, 23, 209 (1973); (b) W. V. Gerasimowicz and J. F. Wojcik, *Bioorg. Chem.*, *11*, 420 (1982)

37. (a) K. A. Connors "Binding Constants", Wiley - Interscience, N. Y., 1987, p.13; (b) *ibid*, p.24; (c) *ibid*, p. 22; (d) *ibid*, p 139; (e) *ibid*, p. 274

38. T. Higuchi and K. A. Connors, *Adv. Anal. Chem. Instr.*, *4*, 117 (1965)

39. T. Rosanske and K. A. Connors, *J. Pharm. Sci.*, *69*, 564 (1980)

40. K. A. Connors, S. Lin, and A. Wong, *J. Pharm. Sci.*, *71*, 217 (1981)

41. K. A. Connors and D. D. Pendergast, *J. Amer. Chem. Soc.*, *106*, 7607 (1984)

42. D. D. Pendergast, Ph.D. Thesis, University of Wisconsin-Madison (1983)

43. S. Lin and K. A. Connors, *J. Pharm. Sci.*, *72*, 1333 (1983)

44. A. Wong, S. Lin, and K. A. Connors, *J. Pharm. Sci.*, *72*, 388 (1983)

45. T. Higuchi and H. Kristiansen, *J. Pharm. Sci.*, *59*, 1601 (1970)

46. K. Kaemi, H Sezaki, T. Mitsunaga, and M. Nakano, *J. Pharm. Sci.*, *59*, 1597, (1970)

47. A. Paulson, M. S. Thesis, University of Wisconsin - Madison (1986)

48. Y. Tamura et al, *Org. Synth.*, *31*, 29 (1951)

49. B. Williamson and W. H. Rodebush, *J. Amer. Chem. Soc.*, *63*, 3018 (1941)

50. N. Kornblum et al, *J. Amer. Chem. Soc.*, *74*, 5782 (1952)

51. C. A. S. Register Number 1591-30-6

VII APPENDICES

A. Computer Program for the Least Squares Analysis of Equation 13

The computer program for the least squares analysis of eq. 13 is reproduced with the solubility data entered for the 4,4'-Dinitrobiphenyl compound as an example. Within the program, [L] is calculated at each experimental L_t according to eq. 14. This program and the program in Appendix B were written on a Digital Equipment Corporation Rainbow computer in BASIC language (47).

```
10      Open "r", 1, "Andrea5.bas"
15      lprint "input values"
        (In lines 20 and 40, I am inputting the beginning estimate of K11 and K12)
20      input "K11 = ";K1
30      lprint "K11 = ";K1
40      input "K12 = ";K2
55      lprint "K12 = ";K2
        (In line 60, I am inputting the number of points)
60      M = 11
        (In line 70, I am inputting the mean experimental So)
70      SO = 0.46E-06
        (In line 75, I am inputting the experimental variance of So)
75      VS = 1.6E-17
80      lprint
85      lprint
90      lprint "LT";TAB(15);"ST exp";TAB(30);"ST calc";TAB(45);"L";TAB(60);
        "(ST - SO) / L"
100     read ST,LT
        (In lines 110 to 180, I am calculating [L] at each experimental Lt, according to
        eq. 14. In line 190, I am renaming [L] as X. Note that [L] is the abcissa of the
        linear equation 13. )
110     A=8*K1*K2*SO*LT
120     B=1 + (K1*SO)
130     C=B^2
140     D=A+C
150     E=SQR(D)
160     F=-B
```

```
170   G=4*K1*K2*SO
180   L=(F+E)/G
190   X=L
      (In lines 205 to 220, I am calculating a "calculated" St at each Lt according to
      eq. 11. These calculated St values will make up the calculated curve)
205   L1=K1*SO*L
210   L2=K1*K2*SO*(L^2)
220   SC=SO+L1+L2
      (In line 700, I am calculating (St - So / [L]), the ordinate of eq. 13.)
700   Y=(ST-SO)/X
705   lprint LT;TAB(15);ST;TAB(30);SC;TAB(45);X;TAB(60);Y
      ( Lines 710 to 836 are the least squares analysis of eq. 13.)
710   X1=X1+X
720   Y1=Y1+Y
730   X2=X2+X*X
740   Y2=Y2+Y*Y
760   P=P+X*Y
770   N=N+1
780   if N<M then goto 100
790   Q=P-((X1*Y1)/N)
800   S=X2-((X1*X1)/N)
802   Z=Q/S
804   W=(Y1-(Z*X1))/N
      (In lines 806 and 808, I am calculating the improved estimates of K11 and K12
      for a single iteration.)
806   K3=W/SO
808   K4=Z/W
812   A1=Y2-((Y1^2)/N)
814   A2=(Q^2)/S
816   A3=A1-A2
818   A4=A3/(N-2)
820   B1=A4/S
822   A6=(X1/N)^2
824   B2=A4*((1/N)+(A6/S))
826   C1=VS/(SO^2)
828   C2=B2/W^2
      (In line 830, I am calculating the standard deviation of K11, according to
      eq. 17.)
830   SJ=(SQR(C1+C2))*K3
832   C3=B1/(Z^2)
      (In line 836, I am calculating the standard deviation of K12, according to
      eq. 18.)
836   SK=(SQR(C2+C3))*K4
840   lprint
843   lprint
```

```
844   lprint "output values"
845   lprint "slope = ";
846   lprint "variance of slope = ";B1
850   lprint "intercept = ";W
851   lprint "variance of intercept";B2
877   lprint
878   lprint
```

(In lines 879 and 882, I am printing the improved values of K_{11} and K_{12} for a single iteration. In lines 880 and 886, I am printing their standard deviations.)

```
879   lprint "K11 = ";K3
880   lprint "std dev K11 = ";SJ
882   lprint "K12 = ";K4
886   lprint "std dev K12 = ";SK
```

(In line 890, I am calculating a_{XX})

```
890   AX=4*(K3/K4)
```

(In line 895, I am printing the improved value of a_{XX})

```
895   lprint "axx = ";AX
```

(In lines 900 to 915, I am calculating the standard deviation of a_{XX}, according to eq. 19)

```
900   Q1=(SK^2)/(K4^2)
905   Q2=(SJ^2)/(K3^2)
910   Q3=SQR(Q1+Q2)
915   SA=Q3*AX
```

(In line 920, I am printing the standard deviation of a_{XX})

```
920   lprint "Saxx = ";SA
```

(In line 940, I am inputting the experimental S_t and L_t as data pairs, i.e. first S_t, L_t, next S_t, L_t, etc.)

```
940   data 0.95E-6,1.2E-3,0.98E-6,1.2E-3,1.29E-6,1.6E-3,1.49E-6,2E-3,1.69E-6,
      2E-3,2.99E-6,4E-3,2.94E-6,4E-3,4.9E-6,6E-3,5.01E-6,6E-3,7.11E-6,8E-3,
      7.65E-6,8E-3<
950   end
```

(Note that this program will perform one iteration only. The program is rerun with the output values from lines 879 and 882 used as input values in lines 20 and 40. The program is rerun until constants K_{11} and K_{12} converge.)

B. Computer Program for First Estimates of K_{11} and K_{12}

To begin the iteration of eq. 13, first estimates of K_{11} and K_{12} are needed. The following program provides those estimates. The basis of the estimate is eq. 15, where the approximation is made that [L] = L_t. The solubility data for 4,4'-Dinitrobiphenyl is entered as an example.

```
10      open "r",1,"andrea6.bas"
50      lprint "(ST-SO)/LT";TAB(20);LT
100     Read ST,LT
        (In line 120, I am inputting the mean experimental So.)
120     SO=0.46E-06
        (In line 125 , I am inputting the number of points.)
125     M=11
        (In line 130, I am calculating the ordinate of eq. 13, but am approximating [L]
        as Lt )
130     Y=(ST-SO)/LT
        (In line 140, I am approximating the abcissa of eq. 13 , [L], as Lt)
140     X=LT
        ( Lines 150 to 250 are the least squares analysis of eq. 13.)
150     X1=X1+X
160     Y1=Y1+Y
170     X2=X2+(X^2)
180     Y2=Y2+(Y^2)
190     P=P+(X*Y)
200     N=N+1
205     lprint Y;TAB(18);X
210     if N<M then goto 100
220     Q=P-((X1*Y1)/N)
230     S=X2-((X1^2)/N)
240     Z=Q/S
250     W=(Y1-(Z*X1))/N
        (In line 260, I am calculating K11, and in line 270, K12. In lines 280 and 290, I
am      printing them.)
260     K1=W/S
270     K2=Z/(K1*SO)
275     lprint "estimate from (ST-SO)/LT vs. LT :"
280     lprint "K11 = ";K1
290     lprint "K12 = ";K2
```

292 lprint

(In line 300, I am inputting the experimental S_t and L_t as data pairs in the form of: first S_t, L_t, next S_t, L_t, etc.)

300 data 0.95E-6,1.2E-3,0.98E-6,1.2E-3,1.29E-6,1.6E-3,1.49E-6,2E-3,1.69E-6, 2E-3,2.99E-6,4E-3,2.94E-6,4E-3,4.9E-6,6E-3,5.01E-6,6E-3,7.11E-6,8E-3, 7.65E-6,8E-3<

400 end

(Note that these estimates will be used as input values in the first iteration of eq. 13. They will be input into lines 20 and 40 in the program in appendix A.)

C. Phase Solubility Diagram for 4,4'–dicarboxybiphenyl with α-Cyclodextrin

The phase solubility diagram for the dicarboxy compound with ligand concentration in the range 0 - 0.004 M was shown in figure 8. Additional studies were done for this system. The equilibrium time was followed by analysis of substrate concentration from samples containing 0.02 M ligand. The results are depicted in figure 16. Samples from different ligand concentrations above 0.004 M were taken after 948 Hr and analysed for total substrate concentration. Figure 17 shows the phase solubility diagram for 4,4' dicarboxybiphenyl with α–cyclodextrin in the range 0 - 0.03 M.

Figure 16

Plot of S_t against time for the 4,4'-dicarboxybiphenyl with 0.02 M α–cyclodextrin.

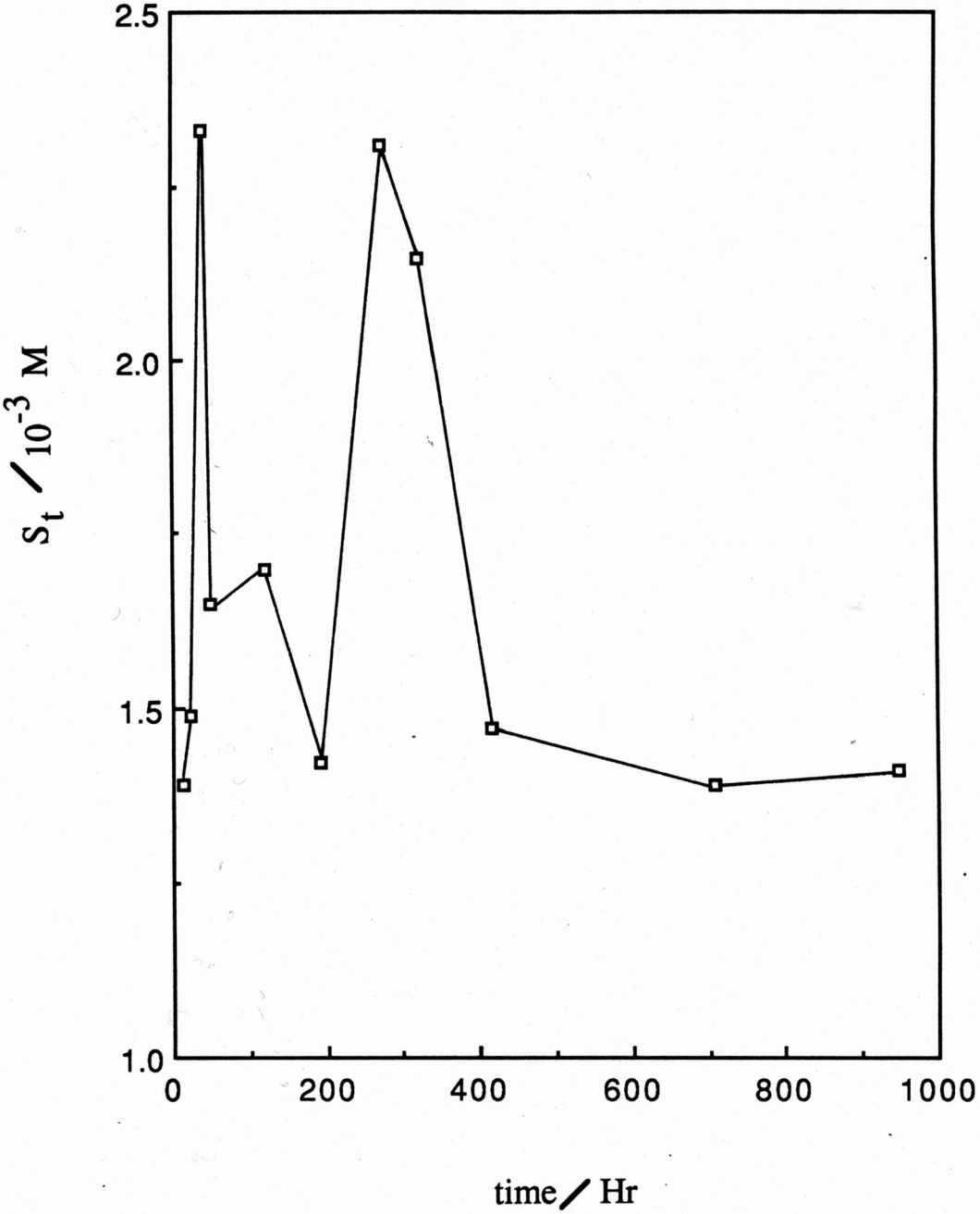
2.5
2.0
1.5
1.0
0
200
400
600
800
1000
S_t / 10^{-3} M
time / Hr

Figure 17

Solubility of 4,4' dicarboxybiphenyl as a function of α–cyclodextrin concentration in the range 0 - 0.03 M, in aqueous solution of 0.01M HCl at 25 °C.

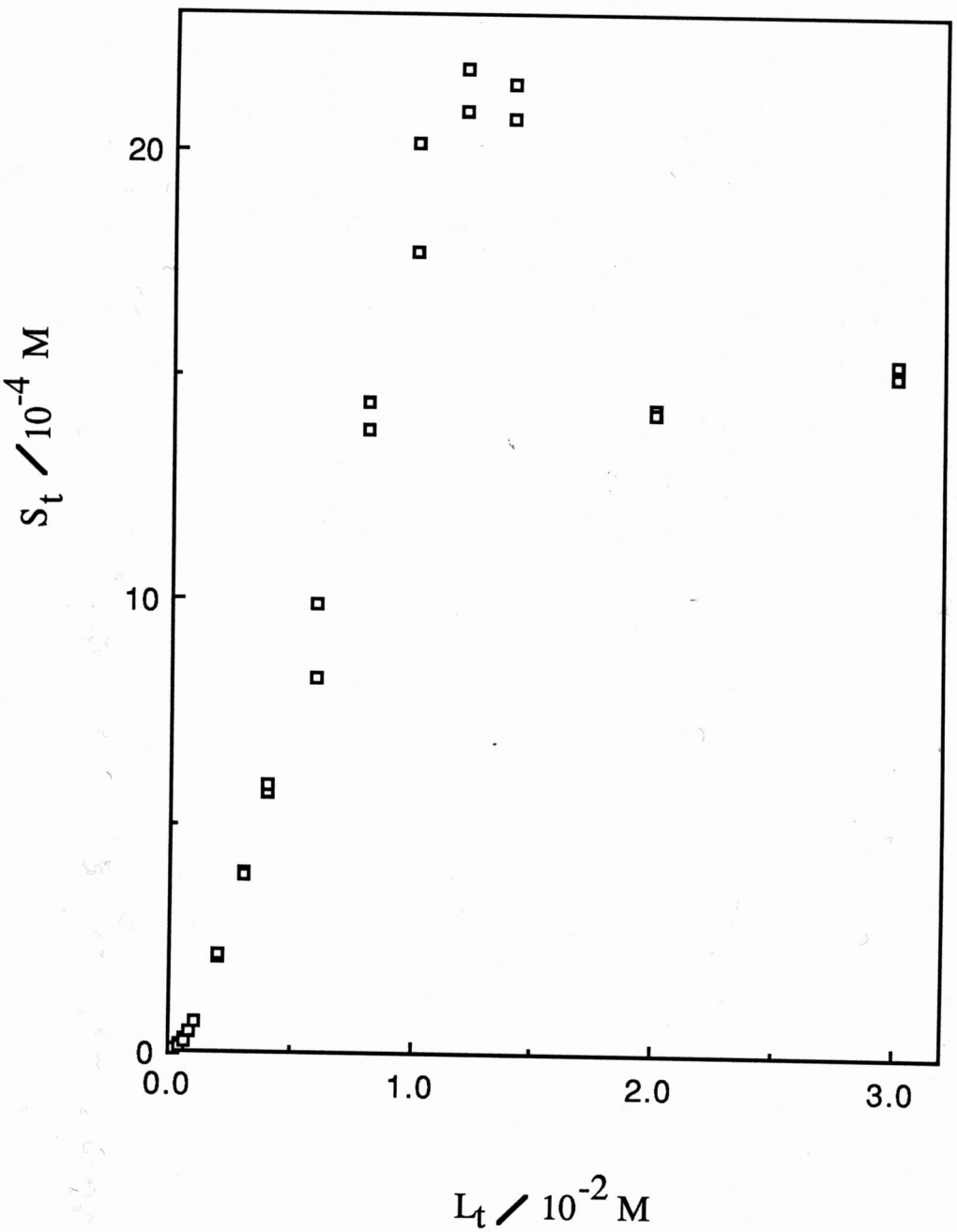
20
10
0
0.0
1.0
2.0
3.0
S_t / 10^{-4} M
L_t / 10^{-2} M

D. Extrapolation estimate of the intrinsic solubility for sym-4,4'-disubstituted biphenyls.

Plot of $\sqrt{S_t}$ against L_t provides a useful extrapolation estimate of the intrinsic solubility value. This type of extrapolation method was done with disubstituted biphenyls, for which S_o was accurately known, to establish the validity of the extrapolation, see figures 18 through 23. Note some of the S_o values may be improved by measuring S_t values at extremely low L_t.

Figure 18

Plot of $\sqrt{S_t}$ against L_t for 4,4'–dinitrobiphenyl. The intercept of the linear regression line provides an extrapolated value of $S_o = 0.049 \times 10^{-5}$ M . The experimental $S_o = 0.046 \times 10^{-5}$ M.

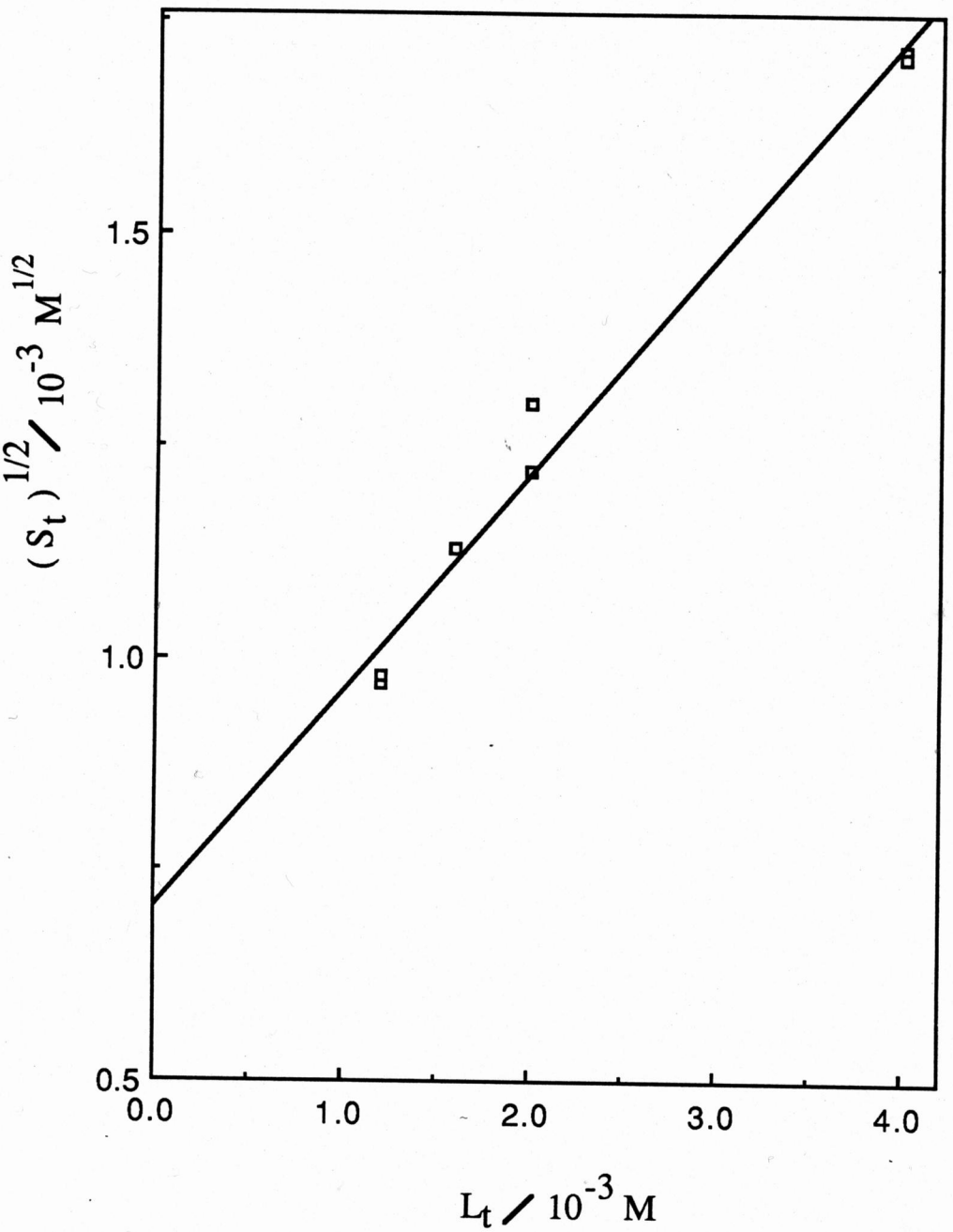
$(S_t)^{1/2} / 10^{-3}\ M^{1/2}$
1.5
1.0
0.5
0.0
1.0
2.0
3.0
4.0
$L_t / 10^{-3}\ M$

Figure 19

Plot of $\sqrt{S_t}$ against L_t for 4,4'-dicarbonitrilebiphenyl. The intercept of the linear regression line provides an extrapolated value of $S_o = 0.506 \times 10^{-5}$ M . The experimental $S_o = 0.507 \times 10^{-5}$ M.

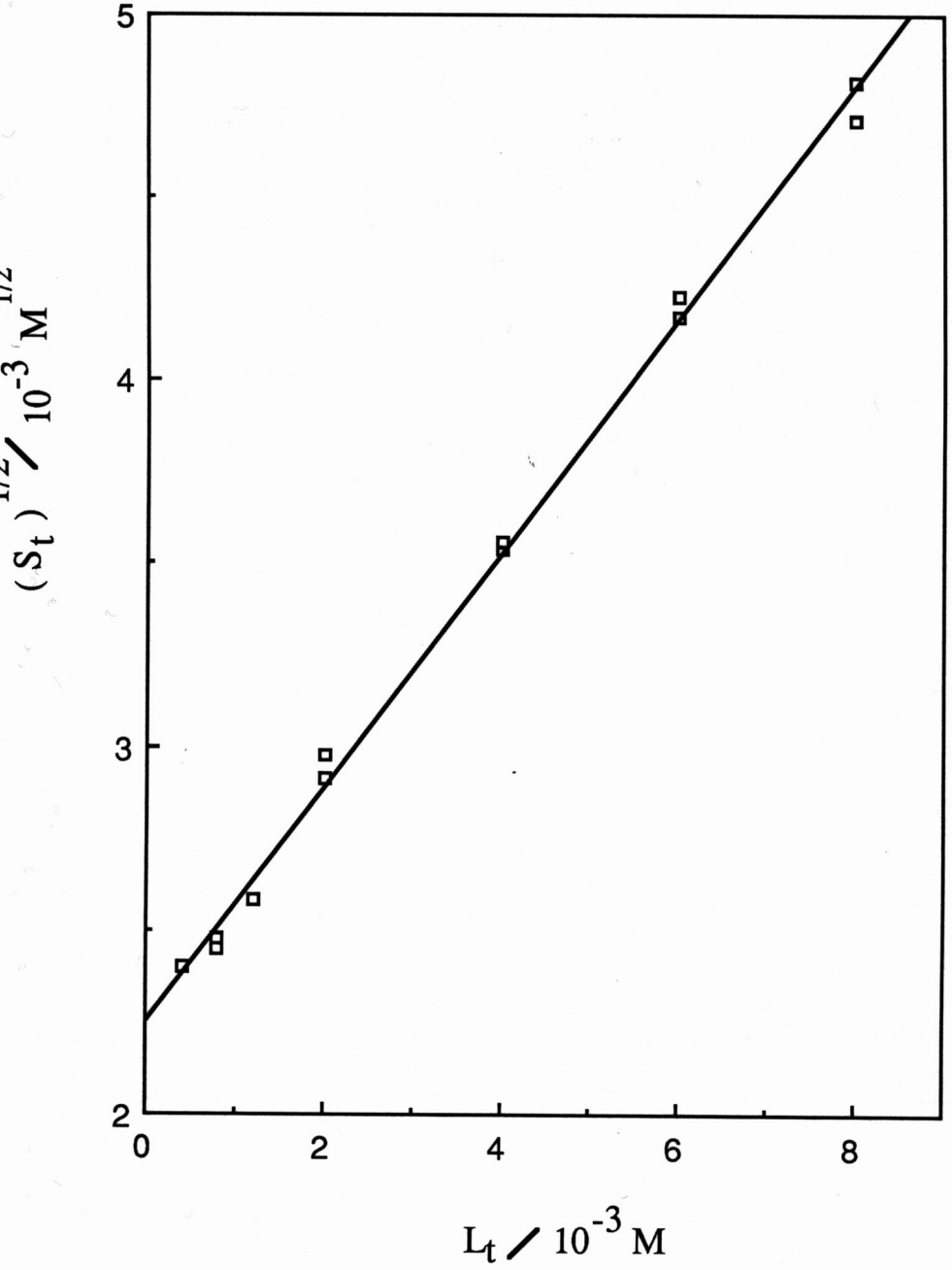
5
4
3
2
0
2
4
6
8
$(S_t)^{1/2} / 10^{-3} M^{1/2}$
$L_t / 10^{-3} M$

Figure 20

Plot of $\sqrt{S_t}$ against L_t for 4,4'-dichlorobiphenyl. The intercept of the linear regression line provides an extrapolated value of $S_o = 0.0098 \times 10^{-5}$ M . The experimental $S_o = 0.026 \times 10^{-5}$ M.

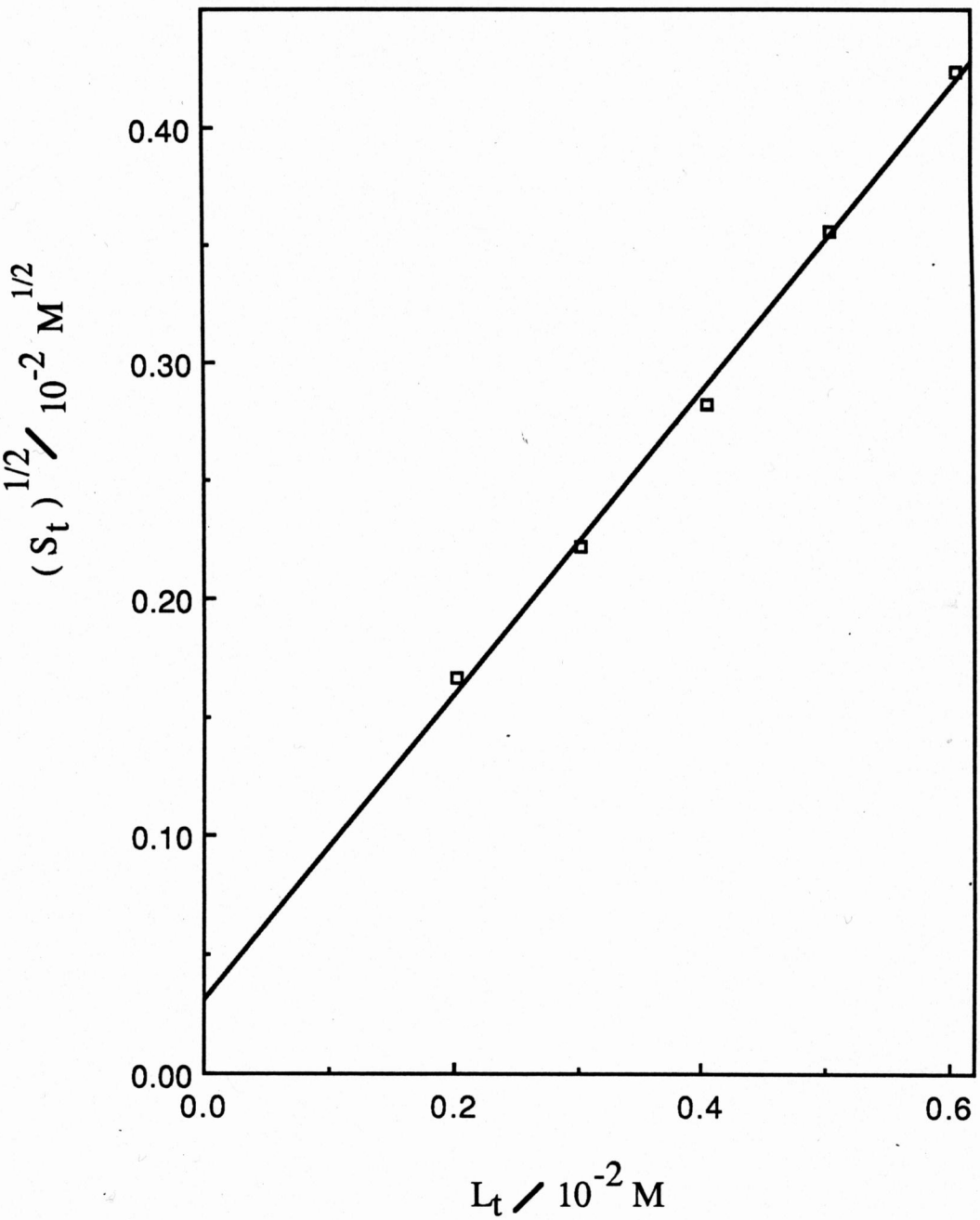
0.40
0.30
0.20
0.10
0.00
0.0
0.2
0.4
0.6
$(S_t)^{1/2} / 10^{-2}\ M^{1/2}$
$L_t / 10^{-2}\ M$

Figure 21

Plot of $\sqrt{S_t}$ against L_t for 4,4'-dimethylbiphenyl. The intercept of the linear regression line provides an extrapolated value of $S_o = 0.10 \times 10^{-5}$ M . The experimental $S_o = 0.054 \times 10^{-5}$ M.

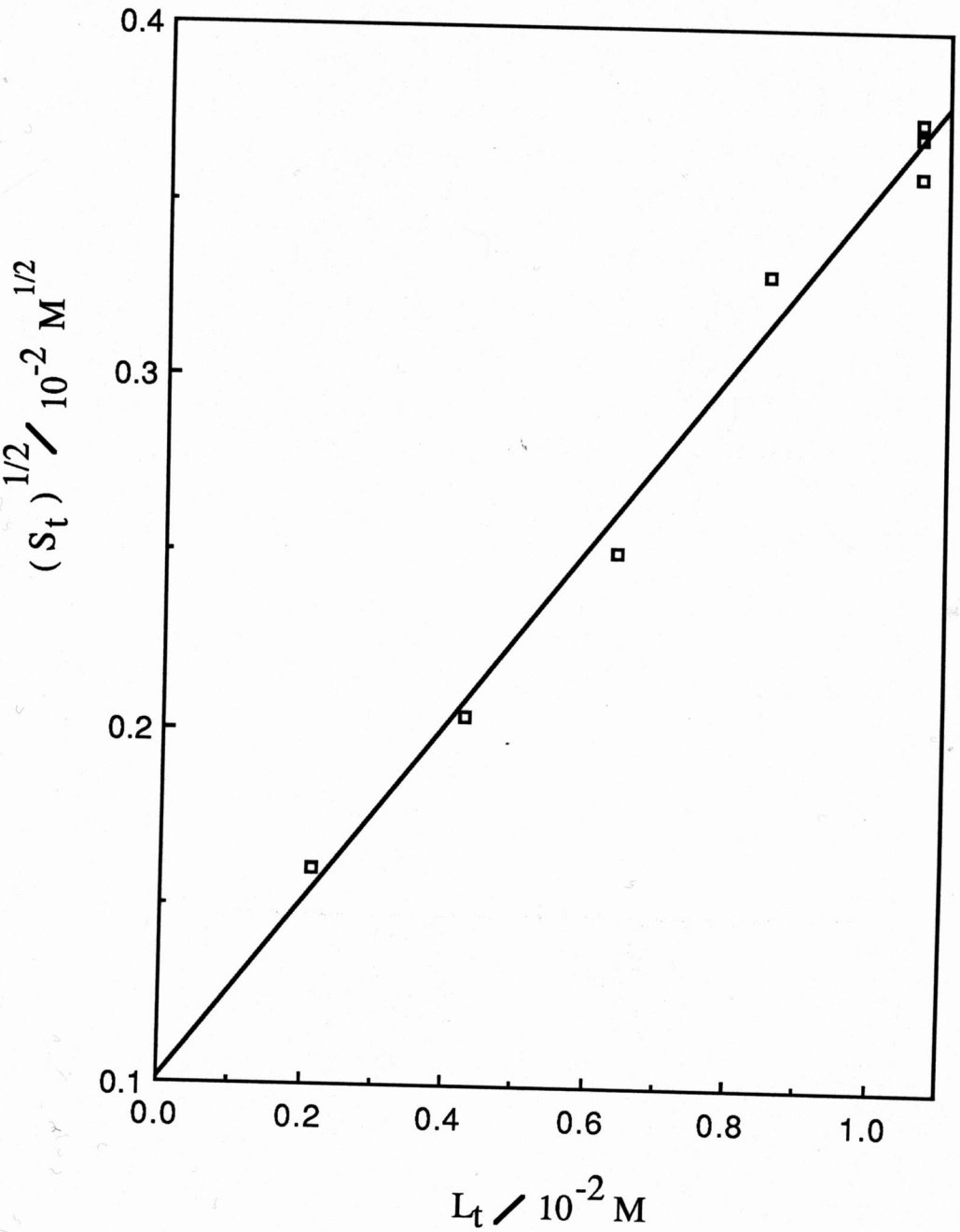
0.4
0.3
0.2
0.1
0.0
0.2
0.4
0.6
0.8
1.0
$(S_t)^{1/2} / 10^{-2} M^{1/2}$
$L_t / 10^{-2} M$

Figure 22

Plot of $\sqrt{S_t}$ against L_t for 4,4'-dihydroxybiphenyl. The intercept of the linear regression line provides an extrapolated value of $S_o = 15.74 \times 10^{-5}$ M . The experimental $S_o = 19.8 \times 10^{-5}$ M.

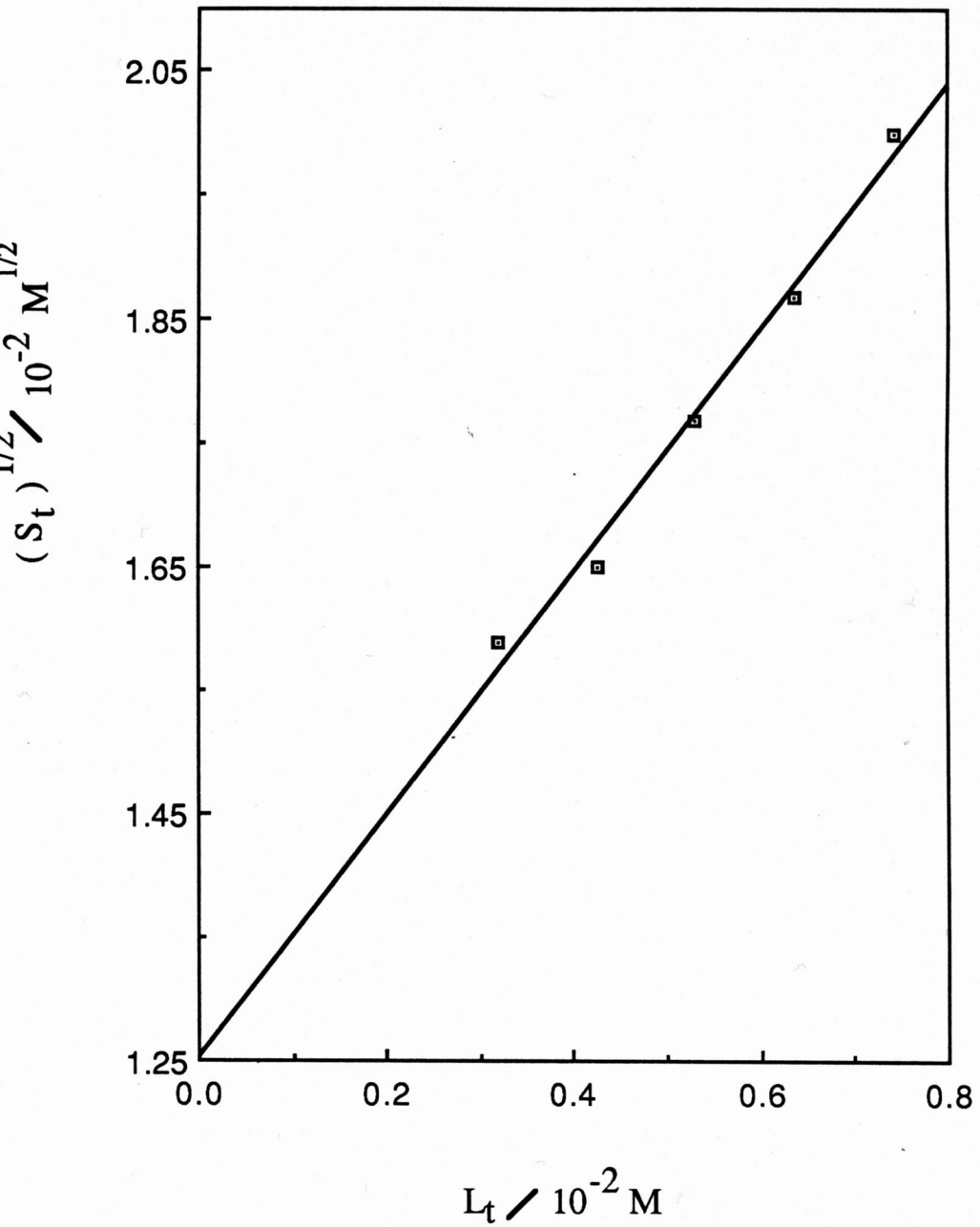
2.05
1.85
1.65
1.45
1.25
0.0
0.2
0.4
0.6
0.8
$(S_t)^{1/2} / 10^{-2} M^{1/2}$
$L_t / 10^{-2} M$

Figure 23

Plot of $\sqrt{S_t}$ against L_t for biphenyl. The intercept of the linear regression line provides an extrapolated value of $S_o = 3.79 \times 10^{-5}$ M. The experimental $S_o = 4.0 \times 10^{-5}$ M.

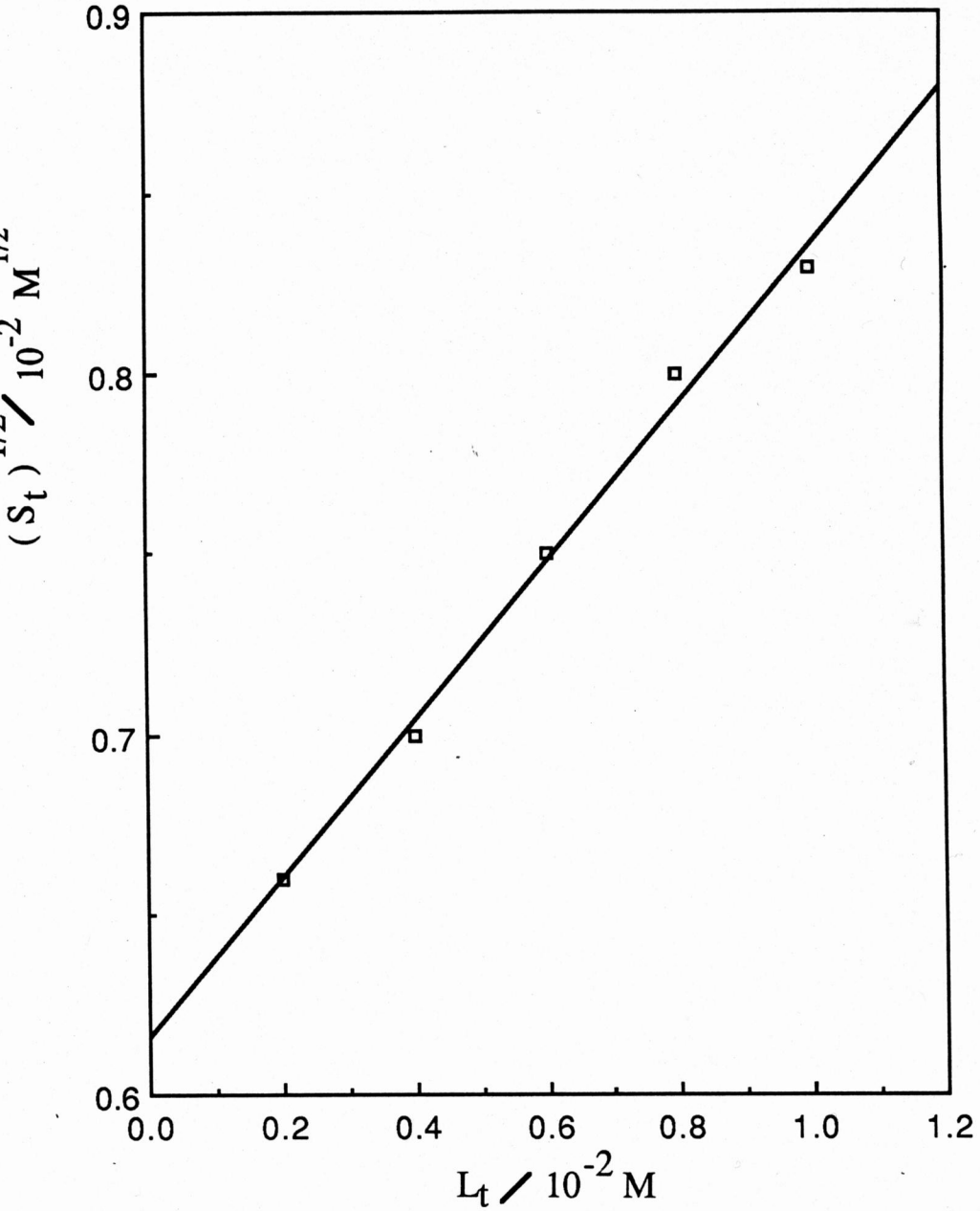
0.9
0.8
0.7
0.6
0.0
0.2
0.4
0.6
0.8
1.0
1.2
$(S_t)^{1/2} / 10^{-2}\ M^{1/2}$
$L_t / 10^{-2}\ M$